



University of Maribor

Faculty of Energy Technology

Journal of ENERGY TECHNOLOGY



Volume 17 / Issue 1

MAY 2024

www.fe.um.si/en/jet.html

Journal of ENERGY TECHNOLOGY



VOLUME 17 / Issue 1

Revija Journal of Energy Technology (JET) je indeksirana v bazah INSPEC® in Proquest's Technology Research Database.

The Journal of Energy Technology (JET) is indexed and abstracted in database INSPEC® and Proquest's Technology Research Database.



JOURNAL OF ENERGY TECHNOLOGY

Ustanovitelj / FOUNDER

Fakulteta za energetiko, UNIVERZA V MARIBORU /
FACULTY OF ENERGY TECHNOLOGY, UNIVERSITY OF MARIBOR

Izdajatelj / PUBLISHER

Fakulteta za energetiko, UNIVERZA V MARIBORU /
FACULTY OF ENERGY TECHNOLOGY, UNIVERSITY OF MARIBOR

Glavni in odgovorni urednik / EDITOR-IN-CHIEF

Jurij AVSEC

Souredniki / CO-EDITORS

Bruno CVIKL
Miralem HADŽISELIMOVIĆ
Gorazd HREN
Zdravko PRAUNSEIS
Sebastijan SEME
Bojan ŠTUMBERGER
Janez USENIK
Peter VIRTič
Ivan ŽAGAR

Uredniško izdajateljski svet / PUBLISHING & EDITORIAL COUNCIL

Dr. Anton BERGANT,
Litostroj Power d.d., Slovenia

Prof. dr. Marinko BARUKČIĆ,
Josip Juraj Strossmayer University of Osijek, Croatia

Prof. dr. Goga CVETKOVSKI,
Ss. Cyril and Methodius University in Skopje, Macedonia

Prof. dr. Nenad CVETKOVIĆ,
University of Nis, Serbia

Prof. ddr. Denis ĐONLAGIĆ,
University of Maribor, Slovenia

Doc. dr. Brigita FERČEC,
University of Maribor, Slovenia

Prof. dr. Željko HEDERIĆ,
Josip Juraj Strossmayer University of Osijek, Croatia

Prof. dr. Marko JESENIK,
University of Maribor, Slovenia

Prof. dr. Ivan Aleksander KODELI,
Jožef Stefan Institute, Slovenia

Prof. dr. Rebeka KOVAČIČ LUKMAN,
University of Maribor, Slovenia

Prof. dr. Milan MARČIČ,
University of Maribor, Slovenia

Prof. dr. Igor MEDVED,
Slovak University of Technology in Bratislava, Slovakia

Prof. dr. Matej MENCINGER,
University of Maribor, Slovenia

Prof. dr. Greg NATERER,
Memorial University of Newfoundland, Canada

Prof. dr. Enrico NOBILE,
University of Trieste, Italia

Prof. dr. Urška LAVRENČIČ ŠTANGAR,
University of Ljubljana, Slovenia

Izr. prof. dr. Luka SNOJ,
Jožef Stefan Institute, Slovenia

Prof. Simon ŠPACAPAN,
University of Maribor, Slovenia

Prof. dr. Gorazd ŠTUMBERGER,
University of Maribor, Slovenia

Prof. dr. Anton TRNIK,
Constantine the Philosopher University in Nitra, Slovakia

Prof. dr. Zdravko VIRAG,
University of Zagreb, Croatia

Prof. dr. Mykhailo ZAGIRNYAK,
Kremenchuk Mykhailo Ostrohradskyi National University, Ukraine

Prof. dr. Marija ŽIVIĆ,
Josip Juraj Strossmayer University of Osijek, Croatia

Tehnični urednik / TECHNICAL EDITOR

Sonja KRAJNC

Tehnična podpora / TECHNICAL SUPPORT

Tamara BREČKO BOGOVČIČ

Izhajanje revije / PUBLISHING

Revija izhaja štirikrat letno v nakladi 100 izvodov. Članki so dostopni na spletni strani revije - www.fe.um.si/si/jet.html / The journal is published four times a year. Articles are available at the journal's home page - www.fe.um.si/en/jet.html.

Cena posameznega izvoda revije (brez DDV) / Price per issue (VAT not included in price): 50,00 EUR.

Informacije o naročninah / Subscription information:
<http://www.fe.um.si/en/jet/subscriptions.html>

Lektoriranje / LANGUAGE EDITING

Shelagh MARGARET HEDGES (EN), AMIDAS d.o.o. (SLO)

Oblikovanje in tisk / DESIGN AND PRINT

Tiskarna Saje d.o.o.

Naslovna fotografija / COVER PHOTOGRAPH

Jurij AVSEC

Oblikovanje znaka revije / JOURNAL AND LOGO DESIGN

Andrej PREDIN

Ustanovni urednik / FOUNDING EDITOR

Andrej PREDIN

Izdajanje revije JET finančno podpira Javna agencija za raziskovalno dejavnost Republike Slovenije iz sredstev državnega proračuna iz naslova razpisa za sofinanciranje domačih znanstvenih periodičnih publikacij / The Journal of Energy Technology is co-financed by the Slovenian Research Agency.

Spoštovani bralci revije Journal of energy technology (JET)

Pred problematiko energetike v Sloveniji je v prihodnjih desetletjih veliko izzivov, na primer: prestrukturiranje energetike v Šaleški dolini, gradnja nove jedrske elektrarne v Krškem, intenzivna uporaba obnovljivih virov energije, intenzivna uporaba vodikovih tehnologij, reševanje ekoloških problemov ... Prav v ta namen bo 21. maja 2024 v Velenju mednarodna konferenca EnRe, ki v svojem imenu združuje besedi energetika in odgovornost (Energy and responsibility). Bistven poudarek na letošnji konferenci bo posvečen iskanju poti do podnebne nevtralnosti in trajnostnega zelenega prehoda. Konferenca bo osredotočena na razvoj in implementacijo inovacij, ki podpirajo preobrazbo energetskih, industrijskih in življenjskih sistemov, s ciljem ustvarjanja trajnostne prihodnosti z neto ničelnimi emisijami. Ta konferenca ne bo zgolj izmenjava znanj, temveč tudi platforma za spodbujanje konkretnih dejanj, ki bodo zagotovila bolj zeleno in trajnostno prihodnost za naše naslednje generacije. Na dogodku bodo sodelovali izkušeni strokovnjaki in študenti s svojimi prispevki. Še posebej zanimiva bodo vabljeni predavanja, ki bodo uvod na okrogli mizi ter posvečena problematiki prenove nacionalnega in podnebne načrta Republike Slovenije ter daljinskemu ogrevanju v Šaleški dolini.

Prepričan sem, da bo konferenca pripomogla k jasnejši sliki energetike v Sloveniji.

Jurij AVSEC
odgovorni urednik revije JET

Dear Readers of the Journal of Energy Technology (JET)

The issue of energy in Slovenia faces many challenges in the coming decades, such as, restructuring of the energy sector in the Šaleška valley, construction of a new nuclear power plant in Krško, intensive use of renewable energy sources, intensive use of hydrogen technologies, solving ecological problems ... The EnRe international conference, which combines the words energy and responsibility in its name, will be held in Velenje on 21. 5. 2024. A significant focus at this year's conference will be devoted to the search for a path to climate neutrality and a sustainable green transition. The conference will focus on the development and implementation of innovations that support the transformation of energy, industrial and living systems, with the goal of creating a sustainable future with net zero emissions. This conference will not only be an exchange of knowledge, but also a platform to promote concrete actions that will ensure a greener and more sustainable future for our next generations. Experienced experts will participate in the event, as well as students with their contributions. The invited lectures will be particularly interesting, as an introduction to the round table, which will be dedicated to the issue of renewing the national and climate plan of the Republic of Slovenia and district heating in the Šaleška Valley. I am convinced that the conference will contribute to a clearer picture of energy in Slovenia.

Jurij AVSEC
Editor-in-chief of JET

Table of Contents

Kazalo

Damage analysis of condenser cooling tubes in thermal power plant Analiza poškodb hladilnih cevi kondenzatorja v termoelektrarni	
Dušan Strušnik, Jurij Avsec	11
Implications for the environmental-engineering compromise as a result of the aftermarket optimization of a diesel engine Posledice za okoljsko-inženirski kompromis zaradi optimizacije dizelskega motorja	
Nikola Manev, Igor Jovchevski, Dame Dimitrovski, Elenior Nikolov	20
Analysis of aged cable` insulation with X-ray fluorescence spectrometry Analiza električne izolacije starih kablov z rentgensko fluoroscenčno spektrometrijo	
Nejc Friškovec, Manja Obreza, Marko Pirc, Klemen Sredenšek, Zdravko Praunseis	32
Conceptual techno-economic analysis of retrofitting a 210 MW thermal heavy-oil power plant with a molten salt thermal energy storage system for renewable power: a case analysis of TEC Negotino Konceptualna tehnno-ekonomska analiza opreme 210 MW termalne elektrarne na težko olje s sistemom za shranjevanje termalne energije s pomočjo staljene soli za obnovljive energije: analiza primera TEC Negotino	
Dragan Minovski, Marija Sterjova	47
Methods for recycling photovoltaic modules and element recovery projections in Slovenia Metode recikliranja fotovoltaičnih modulov in projekcije za pridobivanje elementov v Sloveniji	
Manja Obreza, Nejc Friškovec, Klemen Sredenšek, Sebastijan Seme	61
Instructions for authors	74

DAMAGE ANALYSIS OF CONDENSER COOLING TUBES IN A THERMAL POWER PLANT

ANALIZA POŠKODB HLADILNIH CEVI KONDENZATORJA V TERMoeLEKTRARNI

Dušan Strušnik¹ [✉], Jurij Avsec²

Keywords: ammonia, cooling, cracks, tubes

Abstract

A steam turbine condenser (STC) is a surface, shell, and tube type vacuum condenser, cooled by a water system supplied from a river. The STC consists of two water passes and two water flows. Its condenser shell is constructed from carbon steel, and contains 4910 cooling tubes made of CuZn28Sn1As brass, each with dimensions of 23.0 x 1.0 mm and a length of 6,400 mm.

Three new steam dump devices (SDDs) have been installed on the condenser. Two SDDs are designated for high-pressure (HP) steam, while one is allocated for intermedia-pressure (IP) steam. The primary function of the SDDs is to divert steam from the boiler through the bypass system into the STC. The bypass system is utilised primarily during start-up, shutdown, and for managing excess steam transfer.

The Commissioning and Trials Board conducted tests on the new SDDs, which lasted for five hours. However, during the commissioning phase, high condensate levels in the STC caused trips. Additionally, online monitoring indicated high condensate conductance. Upon opening the condenser water chamber doors and filling the steam side of the condenser with water, it was discovered that twenty-eight of the cooling tubes were leaking. These leaking tubes were subsequently plugged. For further analysis, four cooling tubes were extracted, and two condensate samples were obtained. While extracting the cooling tubes, the other tubes were inspected visually using a borescope to assess their internal condition.

[✉] Corresponding author: Doc. Dr. Dušan Strušnik University of Maribor, Faculty of Energy Technology, Krško, Slovenia, Address, E-mail address: dusan.strusnik1@guest.um.si

¹ University of Maribor, Faculty of Energy Technology, Krško, Slovenia.

² University of Maribor, Faculty of Energy Technology, Krško, Slovenia.

The analysis results indicated that all the cracks on the extracted tubes were located approximately 5 mm from the tube sheet on the front side of the condenser, where the cooling water inlet and outlet are situated. Furthermore, grooves were observed on all the other tubes at the same location, characteristic of stress-corrosion cracking influenced by ammonia.

Povzetek

Kondenzator parne turbine (STC) je površinski, lupinasti in cevni vakuumski kondenzator, hlajen z vodnim sistemom, ki se dovaja iz reke. STC je sestavljen iz dveh vodnih prehodov in dveh vodnih tokov. Ohišje kondenzatorja je izdelano iz ogljikovega jekla in vsebuje 4910 hladilnih cevi iz medenine CuZn28Sn1As, vsaka z dimenzijami 23,0 x 1,0 mm in dolžino 6400 mm.

Na kondenzatorju so bile nameščene tri nove naprave za izpust pare (SDD). Dva SDD-ja sta namenjena za visokotlačno paro (HP), eden pa je dodeljen za paro srednjega tlaka (IP). Primarna funkcija SDD je preusmeritev pare iz kotla skozi obvodni sistem v STC. Obvodni sistem se uporablja predvsem med zagonom, zaustavitvijo in za upravljanje presežnega prenosa pare.

Komisija za zagon in preskušanje je opravila teste novih SDD, ki so trajali pet ur, vendar so med fazo zagona visoke ravni kondenzata v STC povzročile izklope. Poleg tega je spletno spremljanje pokazalo visoko prevodnost kondenzata. Ob odpiranju vrat vodne komore kondenzatorja in polnjenju parne strani kondenzatorja z vodo je bilo ugotovljeno, da pušča osemindvajset hladilnih cevi. Te puščajoče cevi so bile nato zamašene. Za nadaljnjo analizo smo ekstrahirali štiri hladilne cevi in pridobili dva vzorca kondenzata. Med ekstrakcijo hladilnih cevi so bile druge cevi vizualno pregledane z uporabo boroskopa, da se oceni njihovo notranje stanje.

Rezultati analize kažejo, da so vse razpoke na izvlečenih ceveh približno 5 mm od cevne pločevine na sprednji strani kondenzatorja, kjer sta dovod in odvod hladilne vode. Poleg tega so na vseh drugih ceveh na istem mestu opaženi utori, značilni za napetostno korozijsko razpokanje pod vplivom amonijaka.

1 INTRODUCTION

A steam turbine condenser (STC) is a critical component in a power plant's water-steam cycle system. Its primary function is to condense the steam exiting the turbine into water, which can then be pumped back into the boiler to be reheated and reused in the water-steam cycle. Steam from the boiler is directed into the steam turbine, where it expands and generates mechanical energy as it passes through the turbine blades. This energy turns the turbine shaft, which drives a generator to produce electricity. After leaving the turbine, the steam enters the STC at a lower pressure and temperature. Inside the STC, the steam comes into contact with tubes or surfaces cooled by water. This cooling process causes the steam to condense back into water.

The STC bypass system plays a vital role in optimising the performance, stability, and safety of power plant operations by regulating the steam flow through the condenser during various operating scenarios. This system allows for the controlled diversion of steam around the condenser, bypassing the main steam's flow path when necessary. It helps manage the steam flow rates, controls the HP and IP steam pressure, and ensure stable operation during start-up, shutdown, and load changes. The bypass system is complemented by SDDs, which are used to reduce steam pressure before it enters the STC. The SDDs are shown in Fig. 1.

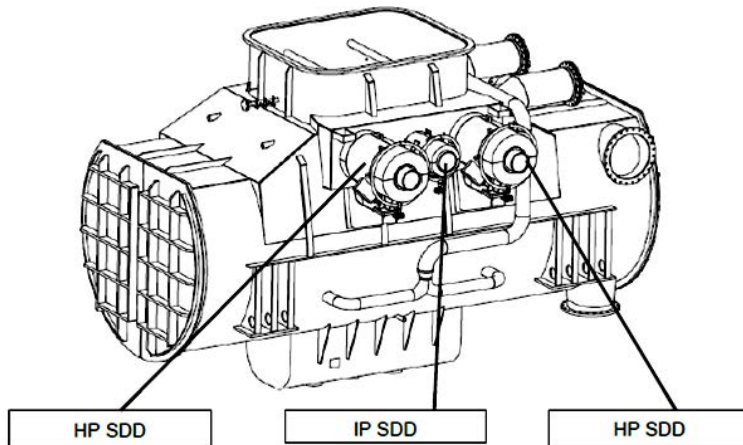


Figure 1: The SDDs integrated on the STC

The STC tube bundle is divided into left and right sides, and each side of the tube bundle are divided into 3 sectors: upper (U), middle (M) and lower (L). The tube bundle sides, tube bundle sector, damaged tubes, and plugged tubes for inspection are shown in Fig. 2.

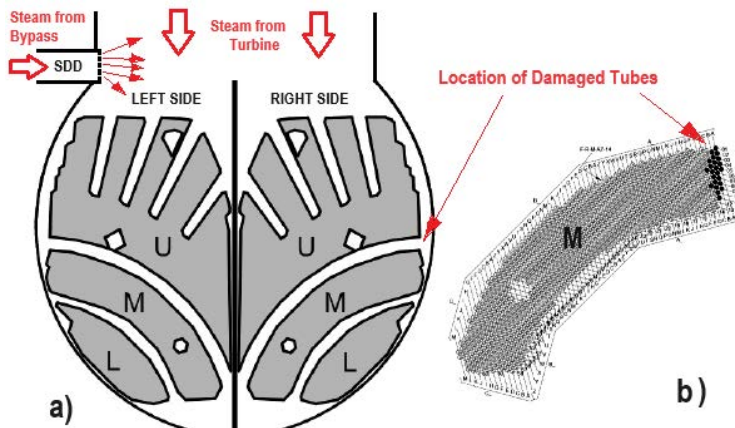


Figure 2. a): Tube bundle sectors, and **b) Damaged tubes and plugged tubes for inspection**

After the fifth hour of test operation, the Commissioning and Trial Board found a leakage in the STC cooling tubes. Additionally, online monitoring indicated high condensate conductance. Two condensate samples were taken from the STC for chemical analysis. One sample was taken before testing, and the second sample was taken during the testing procedure.

For analysis, four cooling tubes were extracted, two condensate samples were obtained, and the steam flow velocity was calculated from the SDDs. While extracting the cooling tubes, other tubes were inspected visually using a borescope to assess their internal condition.

2 RESULTS OF TUBES AND WATER ANALYSIS

All the extracted tubes were examined visually for any cracks or holes. In addition, their inner and outer surfaces were examined, and special attention was given to the outer surfaces of the tubes in places of tube sheets and support plates.

All tubes have a thin, approximately 0.1 mm, nonuniform layer of dry mud spread throughout. This mud layer may be attributed to low cooling water velocity through the condenser tubes, rough filtration of cooling water, or a combination of both factors. Cleaned surfaces show a uniform layer of red-brown oxide, indicating that a naturally forming layer has been established and is serving its purpose of protecting the inner surfaces of the tubes.

All the extracted tubes that were leaking and subsequently plugged were examined, to determine the source of the leaks. Circumferential cracks were found only at the beginning end of the tubes, near the front side. These cracks appeared approximately 3 to 5 mm after the tube sheet and were straight or slightly branched. Additionally, grooves were discovered on other tubes in the same location as the cracks found on the leaking tubes. These circumferential transverse grooves near the tube sheets are indicative of trans-granular stress-corrosion cracking, likely caused by excessive ammonia. The location of tube cracking and the cracks on the front end of the tube are show in Fig. 3.

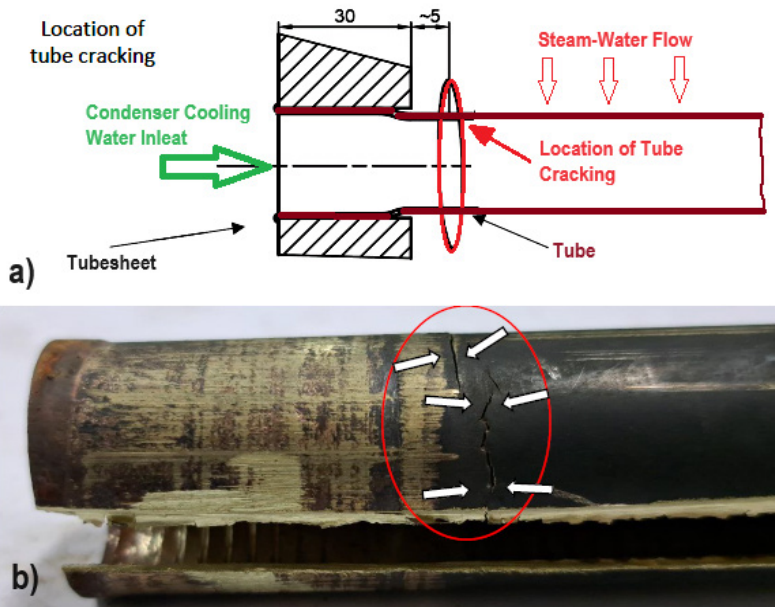


Figure 3. a): Location of tube cracking and **b) Crack** on the front end of the tube, approximately 5 mm after the tube sheet

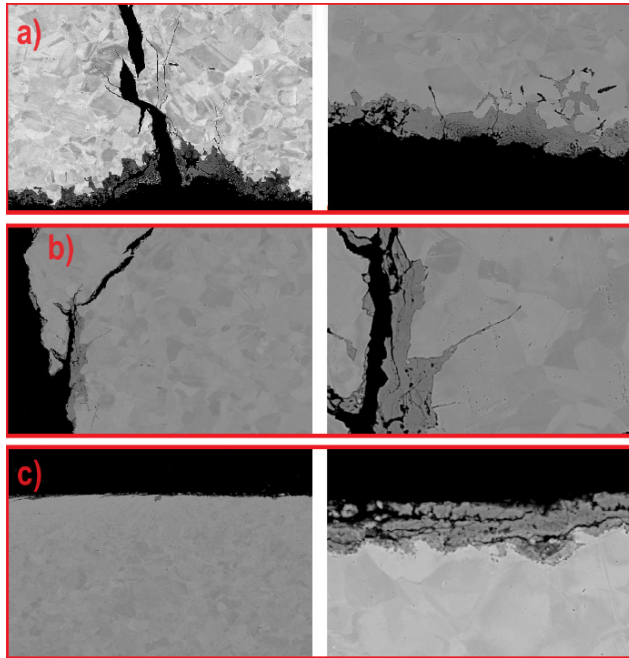


Figure 4: Examination under a microscope revealed: a) Transcrystalline progression, b) Additional cracks branching from the main crack, and c) Oxidation on the outer surface

Analysis of the tube also involved examination under a microscope. From Fig. 4, the following observations were made:

- a) The initiation of cracks on the inner surface of the pipe;
- b) The presence of multiple transcrystalline cracks;
- c) Oxidation of the outer surface with no visible marks;
- a) and b) Branched secondary cracks observed adjacent to the main crack and
- a), b) and c) Oxidation to a thickness of 50 μm .

Also, two condensate samples were provided for chemical analysis. The results of the chemical analysis of the condensate are presented in Table 1, along with the safe operating values for steam turbine steam-water cycles where heat exchangers with brass tubes are installed.

Table 1: Chemical analysis of the condensate

No.	Sample name	pH	λ Electrical conductivity ($\mu\text{S}/\text{cm}$)	NH3 Ammonia (ppb)
1	Before start	8.2	59.3	6135
2	During operation	9.6	7.8	1827
a	Values considered safe during commissioning	Min. 5.0	Max. 1.0	Max. 1000
b	Values considered safe during normal plant operating modes	9.0 to 9.3	Max. 0.25	250 to 700

From the results of the analyses, it can be summarised that the cracks initiated on the inner surface of the tube and progressed transcrystallinely throughout. Multiple visible cracks were observed, characterised by branching and the presence of oxides, which are common indicators of stress corrosion cracking.

All the cracks on the tubes that were extracted were found at the same position, approximately 5 mm from the tube sheet on the front side of the condenser, where the cooling water inlet and outlet are located. Grooves were also found on all other tubes at the same location, characteristic of stress-corrosion cracking influenced by ammonia.

These cracks and grooves were found primarily in places where the tubes were rolled into the tube sheets, indicating high stress. It is assumed that these grooves may also be caused by stress corrosion cracking under ammonia, but were either self-healed, or had not progressed to cracks yet.

No other areas on the tubes showed signs of damage, and there were no damages on the tubes where the tube bundle support plates are located. Chemical analysis of the condensate samples revealed an extremely high concentration of ammonia.

3 RESULTS OF THE HP SDDs PERFORMANCE ANALYSIS

In addition to analysing the STC tubes and condensate quality, we also conducted a performance analysis of the HP SDDs. We obtained data on the quality and quantity of steam entering the HP SDDs device using the Supervisory Control and Data Acquisition (SCADA) system (see Fig. 5).

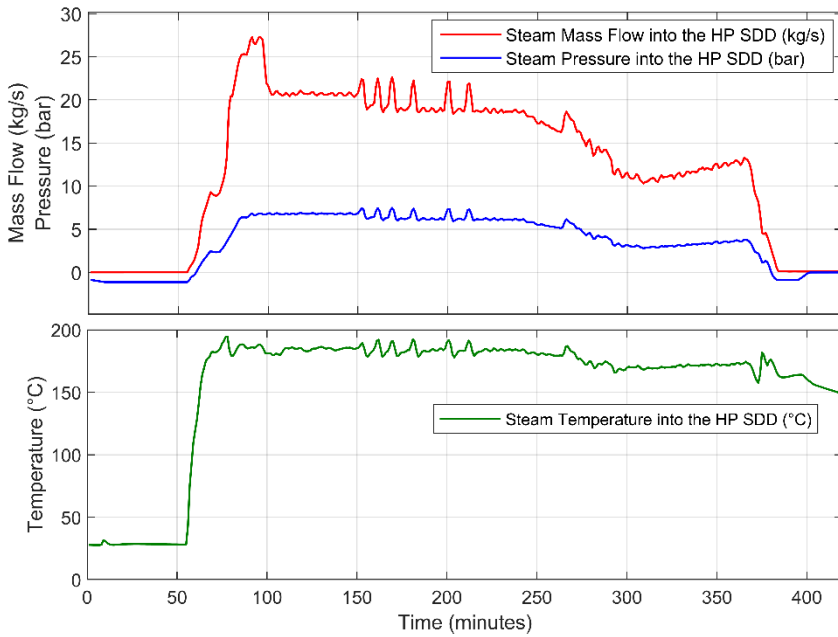


Figure 5: Quality and quantity of steam entering the HP SDDs device

Fig. 5 illustrates that, during HP SDD device operation, the incoming steam reached a maximum flow rate of 26 kg/s, with a pressure of up to 9 bar and a temperature of up to 190°C. The steam exit velocity from the HP SDD device, also known as the steam velocity entering the STC, was calculated using these data. The steam velocity from the HP SDD device was calculated using the Mach number equation. The steam Mach number is defined from the total pressure difference of the dumped steam flow and the isentropic exponent n . The velocity is calculated of the steam exiting the HP SDD device:

$$v_4 = M \cdot v_{SS} = \sqrt{\frac{2}{n-1} \cdot \left(\left(\frac{p_3}{p_4} \right)^{\frac{n-1}{n}} - 1 \right)} \cdot v_{SS} \quad (3.1)$$

where v_4 is the velocity of the steam exiting the HP SDD device, M is the Mach number, v_{SS} is the sound speed of the steam, p_3 is the steam pressure in the rear chamber of the HP SDD device, p_4 is the steam pressure entering the STC, and n is the isentropic exponent. The results of the steam speed calculation from the HP SDD, depending on the load, are shown in Fig. 6.

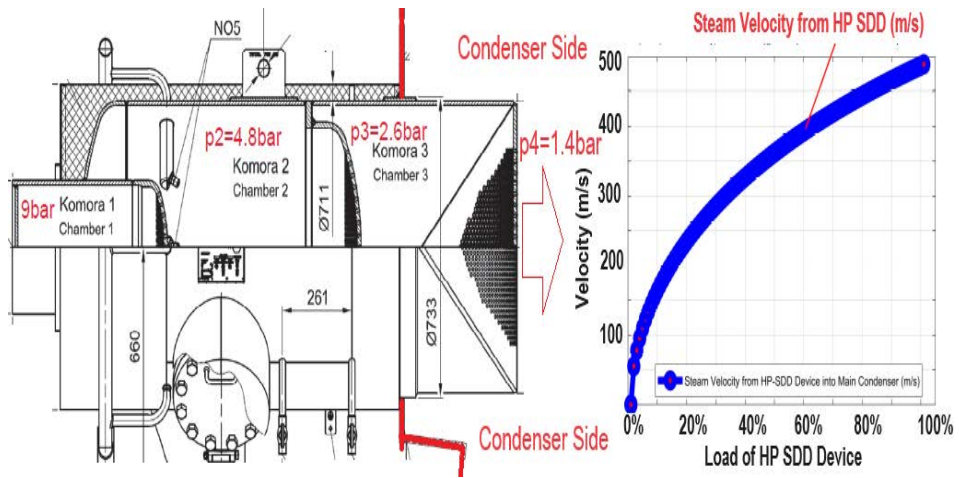


Figure 6: Design and steam velocity from the HP SDD

The results of the analysis (see Fig. 6) show that, at full load of the HP SDD, the steam velocity entering the STC was 490 m/s, exceeding the recommended steam velocities significantly. Bypass steam with excessive velocities can cause severe damage to the condenser internals. The Heat Exchange Institute (HEI) Standards for steam surface condensers provide limits for maximum enthalpy, pressure, and velocity of bypass drain or bypass steam allowed to enter into the condenser. According to the HEI, the maximum enthalpy is 2850 kJ/kg, the maximum pressure is around 18 bar, and the maximum steam velocity is around 155 m/s. Wet steam is not permitted. Damaged bypass headers, sheared tubes, and damage to internal structural members have been encountered frequently during bypass operation.

4 CONCLUSIONS

Based on the results of the analysis, it can be concluded that the damage to the STC cooling tubes was attributed to a combination of circumstances that led to stress corrosion cracking. Excessive steam inlet velocities in the STC caused large surface and resonance loads on the cooling tubes. Additionally, the excessive amount of ammonia in the condensate contributed to surface corrosion. As the cracks propagate from the inner tube to the outside, it is necessary to maintain a constant flow of cooling water.

Measures to prevent damage to the STC tubes:

- About three rows of tubes around the affected area, including the affected area, should be replaced with thicker tubes, 23.0 x 2.0 CuZn28Sn1As;
- The ammonia content in the steam should be monitored carefully, and should be kept to 250 ppb up to 700 ppb, and the pH maintained between 9.0 and 9.3;
- The steam velocity from the SDDs should be reduced to the HEI recommended velocity.

References

- [1] **D. D. Van Slyke.** The Analysis of Proteins by Determination of the Chemical Groups Characteristic of the Different Amino-Acids. *A journal of the American Society for Biochemistry and Molecular Biology*, Pages 15-55. [https://doi.org/10.1016/S0021-9258\(18\)91437-7](https://doi.org/10.1016/S0021-9258(18)91437-7)
- [2] **T.S Rao, K.V.K Nair** (1998). Microbiologically influenced stress corrosion cracking failure of admiralty brass condenser tubes in a nuclear power plant cooled by freshwater. *Corrosion Science*, 40, Issue, 1821-1836 [https://doi.org/10.1016/S0010-938X\(98\)00079-1](https://doi.org/10.1016/S0010-938X(98)00079-1)
- [3] **E. Sharifi, K. Ranjbar** (2022). Dezincification assisted cracking of yellow brass tubes in a heat exchanger. *Engineering Failure Analysis*, 136, 2022, 106200 <https://doi.org/10.1016/j.engfailanal.2022.106200>
- [4] **Yong-De Li, Na Xu, Xiao-Feng Wu, Wei-Min Guo, Jun-Bo Shi, Qi-Shan Zang** (2013) Failure analysis of the condenser brass tube in 150 MW thermal power units. *Engineering Failure Analysis*, 33, 75-82 <https://doi.org/10.1016/j.engfailanal.2013.04.026>
- [5] **S.R. Kaji, N.P. Gulhane** (2017). Desig of steam dump device for steam surface condensers. *International Journal of Management and Applied Science*, 3, 2394-7926. https://www.ijraj.in/journal/journal_file/journal_pdf/14-407-151159289187-91.pdf Heat Exchange Institute, Inc., "Standards for Steam SurfaceCondensers", 11th Edition, September, 2012
- [6] **R.K.Rajput**, "Thermal Engineering", Laxmi Publications, 2010
- [7] **S.K.Som, G. Biswas, and S. Chakraborty**, "Introduction to Fluid Mechanics and Fluid Machines", Third Edition,Mc-Graw-Hill, 2008
- [8] **D. M. Nightingale**, "Thermal & Mechanical Design Guidelines and General Considerations for the Proper Design, and Location, of Various Types of Service Connections on Steam Surface Condensers" Proceedings of the ASME 2015 Power Conference, San Diego, California, 2015

IMPLICATIONS FOR THE ENVIRONMENTAL-ENGINEERING COMPROMISE AS A RESULT OF THE AFTERMARKET OPTIMIZATION OF A DIESEL ENGINE

POSLEDICE ZA OKOLJSKO-INŽENIRSKI KOMPROMIS ZARADI OPTIMIZACIJE DIZELSKEGA MOTORJA

Nikola Manev^{1✉}, Igor Jovchevski², Dame Dimitrovski², Elenior Nikolov¹

Keywords: calibration, tuning, fuel prices, performance, fuel consumption

Abstract

New IC engines contain many systems that ensure better engine performance, while satisfying increasingly strict environmental norms and exhaust emission standards in what is known as an environmental-engineering compromise. However, controlling, calibrating, and subsequently optimizing high-performance engines in which the trade-offs between performance, economy and emissions take precedence, is a challenge for even the most experienced automotive engineers, as it includes major implications. With the rise of fuel prices however, in recent years, more and more transport companies and fleet owners have looked to improve their vehicles' economy through different aftermarket optimizations of the vehicles' engines, rarely

^{1✉} Corresponding author: Teaching assistant Nikola Manev, Ph.D., University "Goce Delcev" - Stip, Military academy "General Mihailo Apostolski" - Skopje, Vasko Karangeleski, bb, Skopje, E-mail address: nikola.manev@ugd.edu.mk

1 University "Goce Delcev" - Stip, Military academy "General Mihailo Apostolski" - Skopje, Vasko Karangeleski, bb, R. N. Macedonia

2 University of "Ss. Cyril and Methodius" in Skopje, Faculty of Mechanical Engineering, Rugjer Boskovic 18, P.O. Box 574 1000 Skopje, R. N. Macedonia

taking into account the impact of such changes on the overall balance imposed through the environmental-engineering compromise. This paper investigates the required changes into the engines' electronic control units to achieve higher power output and lower fuel consumption, while analyzing the benefits and shortcomings brought by these optimizations on the engines' short and long-term operation.

Povzetek

Novi motorji z notranjim zgorevanjem imajo številne sisteme, ki zagotavljajo boljše delovanje, hkrati pa izpolnjujejo vse strožje okoljske norme in standarde emisij izpušnih plinov v tako imenovanem okoljsko-inženirskem kompromisu. Vendar so krmiljenje, umerjanje in posledično optimiziranje visokozmogljivih motorjev, pri katerih imajo prednost kompromisi pred zmogljivostjo, ekonomičnostjo in emisijami, izziv tudi za najbolj izkušene avtomobilске inženirje. Zaradi dviga cen goriva si v zadnjih letih vse več prevoznških podjetij in lastnikov vozniških parkov prizadeva izboljšati ekonomičnost svojih vozil z različnimi poprodajnimi optimizacijami motorjev vozil, pri čemer le redko upoštevajo vpliv takih sprememb na splošno ravnotežje, uvedeno s kompromisom okoljskega inženiringa. Ta prispevek raziskuje potrebne spremembe v elektronskih krmilnih enotah motorjev za doseganje večje izhodne moči in manjše porabe goriva, hkrati pa analizira prednosti in pomanjkljivosti, ki jih prinašajo te optimizacije na kratkoročno in dolgoročno delovanje motorjev.

1 INTRODUCTION

In the 1980s road transport started bringing up major environmental concerns which have gained in relevance continuously [1-2], so most Western European countries, USA, Japan and others, started introducing maximum allowable concentrations of the exhaust emissions of internal combustion (IC) engines, first limiting their exhaust opacity, and later introducing limits on the quantity of: carbon monoxide (CO), carbon dioxide (CO₂), nitrogen oxides (NO_x), particulate matter (PM), sulfur dioxide (SO₂), volatile compounds (VOCs), and unburned fuel [3]. Today, IC engines contain many electronically controlled systems that ensure better engine performance, while satisfying the increasingly strict environmental norms and exhaust emissions standards in what is known as an environmental-engineering compromise. The technological advances toward cleaner combustion at the very least include high-pressure fuel injection, exhaust gas recirculation, turbocharging and cooling the air ahead of the intake manifold [4]. This brings up the complexity of engine control, since each additional system increases the number of inputs in the control matrix, which possess a challenge for fast calibration and optimization of the engine's working parameters, which, in turn, is indivisible from new engine design [5-7].

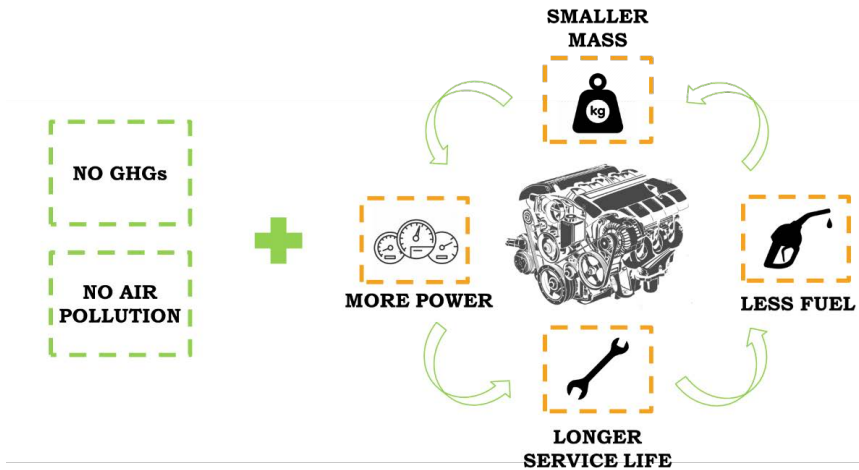


Figure 1: The environmental-engineering compromise

Fuzzy-logic control and altering the control maps in the engine's electronic control unit (ECU) also offer tempting aftermarket performance opportunities [8]. Although tuning an engine, along with other physical engine modifications is almost standard practise with automotive enthusiasts, more recently its application has gained in popularity with transport companies with large vehicle fleets, and even private owners looking to gain the most out of their vehicles [9]. In fact, one of the most recurring control modifications offered by licensed services (and often unlicensed servicing entities as well), is the possibility to increase engine power and torque while reducing fuel consumption [10], also known as POWER and ECONOMY optimizations.

In the available referent literature, [11] analyzes the different aftermarket engine calibration approaches available, while [12] reports on the use of a fuzzy logic controller to maintain engine operation within the most optimal boundaries, but none provide input on the subsequent implications or drawbacks associated with these approaches. Reference [13] is more thorough in this aspect, by proposing a new tuning method and listing its commercial benefits. However, it does not cover the challenges that such modifications bring, such as their impact on the engine components' life or exhaust emissions' quantities. Reference [14] reviews multiple studies of engine calibration problems from the perspective of optimization of three different engines (gasoline, diesel and hybrid), and suggests a more efficient approach to engine calibration. Although the article covers the research on both off-board and on-board engine calibration, it fails to identify the parameters and quantify the results that indicate the negative impact of the procedure.

While soaring fuel prices brought by the ongoing conflict in Ukraine have acted as a catalyst for transport companies and fleet owners to look into increasing their vehicles' economy through aftermarket optimization, account is rarely taken of the potentially negative impact of such modifications. With this in mind, this paper's aim is to detail the required changes in the engine and its system's operation, and understand and quantify both the advantages, but, foremost, the disadvantages in terms of exhaust emissions and engine service life following aftermarket POWER and ECONOMY optimizations of a diesel engine's operation.

2 MATERIALS & METHODS

2.1 Test engine

Passenger vehicles in the Western Balkans (Albania, Bosnia and Herzegovina, Kosovo, North Macedonia, Montenegro and Serbia) have an average age of just above 11 years, with the share of new vehicles being particularly low [15]. With legislative restrictions in place on importing passenger vehicles driven by IC engines that do not comply with the Euro 4 environmental Standards, it is safe to say that most vehicles found within this region will be driven by IC engines that fall within the Euro 4 bracket, or on the transition to Euro 5 [16]. The research and testing is performed on a sufficiently modern diesel engine - the 1.9 dm³, in-line, four-cylinder, four stroke, turbocharged direct injection (TDI) engine, manufactured by the VW group from 2005-2009. It employs such technological advancements as direct injection, a variable turbine geometry turbocharger, a charge intercooler, water-cooled exhaust gas recirculation and a BOSCH EDC 16 electronic control unit.

The vehicle used for the purpose of the research was a SEAT Leon Mk2 driven by the 1.9 TDI engine, which, in its factory setting, can deliver 78 kW of power at 4000 rpm and 250 Nm of torque at 2300 rpm. (Figure 2) Additionally, its combined fuel economy (urban and highway) is 6.6 l/100 km (Figure 3). Furthermore, upon measuring the quantity of the different components found in the vehicle's exhaust emissions that fall under the legal frameworks of the Republic of North Macedonia, and, in particular, the Rule book for the technical inspection of vehicles [17] in the Republic of North Macedonia, per its factory settings, the engine emits 3.43% of CO₂ per volume of exhaust emissions.

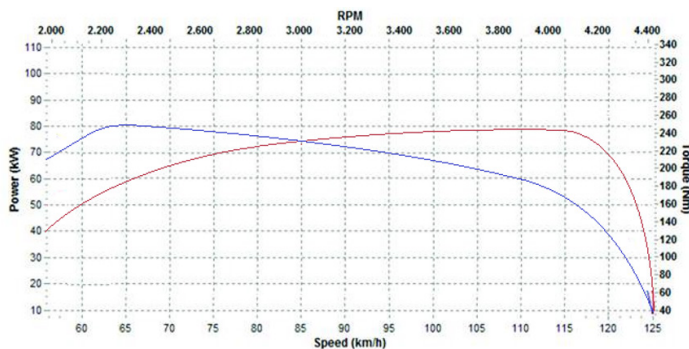


Figure 2: Power and torque curves of the non-optimized 1.9 TDI engine (Engine ID Code: BKC/BLS BXE)



Figure 3: Fuel consumption per the engine's factory settings (board computer read out)

2.2 Testing and measuring equipment

The equipment used to monitor and measure the engine's output operational characteristic has included the TEXA SpA IDC 5 Car diagnostics software and Ross-Tech's VCDS diagnostics software for vehicles of the VW group. Both softwares are suitable for technicians familiar with the basics of self-diagnosis, as these toolkits provide the most detailed techniques for the most advanced

features available with the new generations of electronic control units adopted on most modern vehicles. Aside from their monitoring and diagnostics capability, the VCDS software was also used to perform the tuning and optimization of the operating parameters of the Seat Leon's 1.9 TDI engine, to achieve better engine performance and reduced fuel consumption. Although the TEXA IDC 5 also allows performing permanent adjustments or reprogramming some actuators through the functions provided by the control unit, this software was used primarily to monitor the engine data once the optimizations were completed. Additionally, a BrainBee AGS 688 Gas Analyzer (Figure 4) equipped with an exhaust probe (Figure 5), was used to measure and compare the before and after emissions' footprint of the test-engine.



Figure 4: BrainBee AGS 688 Gas Analyzer



Figure 5: Exhaust probe

2.3 Optimization of the engine's output operating characteristics

Car manufacturers base their engines' ECUs on fuzzy logic, and the BOSCH EDC 16 ECU paired with the 1.9 TDI engine is no exception. The fuzzy logic maps used as lookup tables within the ECU hold predetermined values that the engine should achieve, namely, power (kW), torque (Nm) and the quantity of pollutants in the exhaust emissions, expressed as a percentage (%) of the volume of total exhaust emissions. All the maps are uploaded to a .hex file (HEX – hexadecimal source file) within the ECU's EEPROM (electrically erasable programmable read-only memory), but to get them to the desired state requires hard work and many precise calculations (as a safety measure that protects the manufacturer from amateurs damaging the engine and causing expensive and often irreversible defects).

Performing the ECONOMY and POWER aftermarket engine optimizations includes changing more than 50 control surfaces or maps, only a part of which will be provided in this paper. To achieve reduced fuel consumption and CO₂ emissions, the goal of these optimizations is to increase engine power for the same amount of fuel (Figure 6) that would be injected into the non-optimized engine. Practically, this would mean that the engine would consume less fuel to overcome the same resistance (the sum of forces that oppose the vehicle's motion), and, consequently, it would lead to lower CO₂ emissions. This optimization also requires advancing the start of injection (Figure 7), but, at most, up to 20° BTDC, since, according to [18-19], the consequences of early injection will lead to engine knock, and a significant increase in combustion temperature.

Implications for the environmental-engineering compromise as a result of the aftermarket optimization of a diesel engine

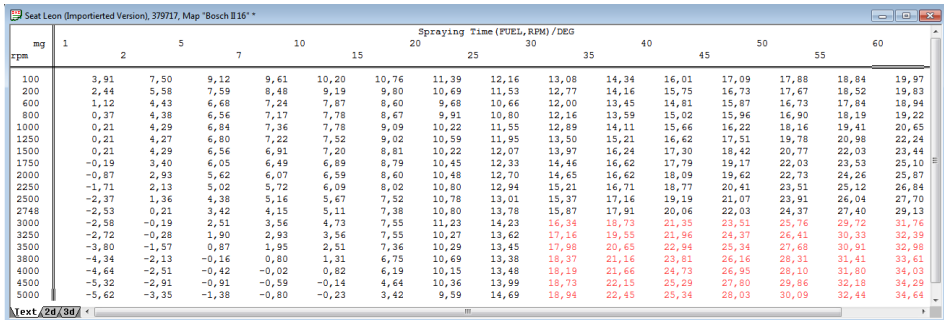


Figure 6: ECONOMY optimization – Injection duration (Fuel, RPM/DEG)

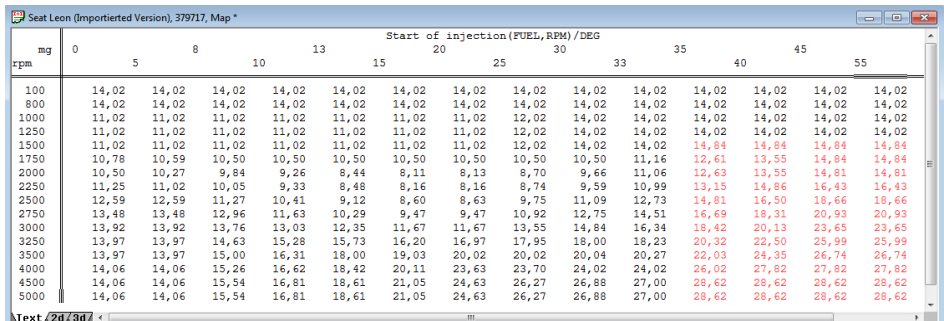


Figure 7: ECONOMY optimization – Start of Injection (Fuel, RPM/DEG)

However, the output engine power can be increased further by changing the angle of attack of the variable geometry turbine blades. Reducing the cross-section of the exhaust gas flow to the turbine will result in a higher speed of the exhaust gas flow, which will lead to a higher rotational speed of the turbocharger, and an increase in the boost pressure and the density of the intake charge (Figure 8).

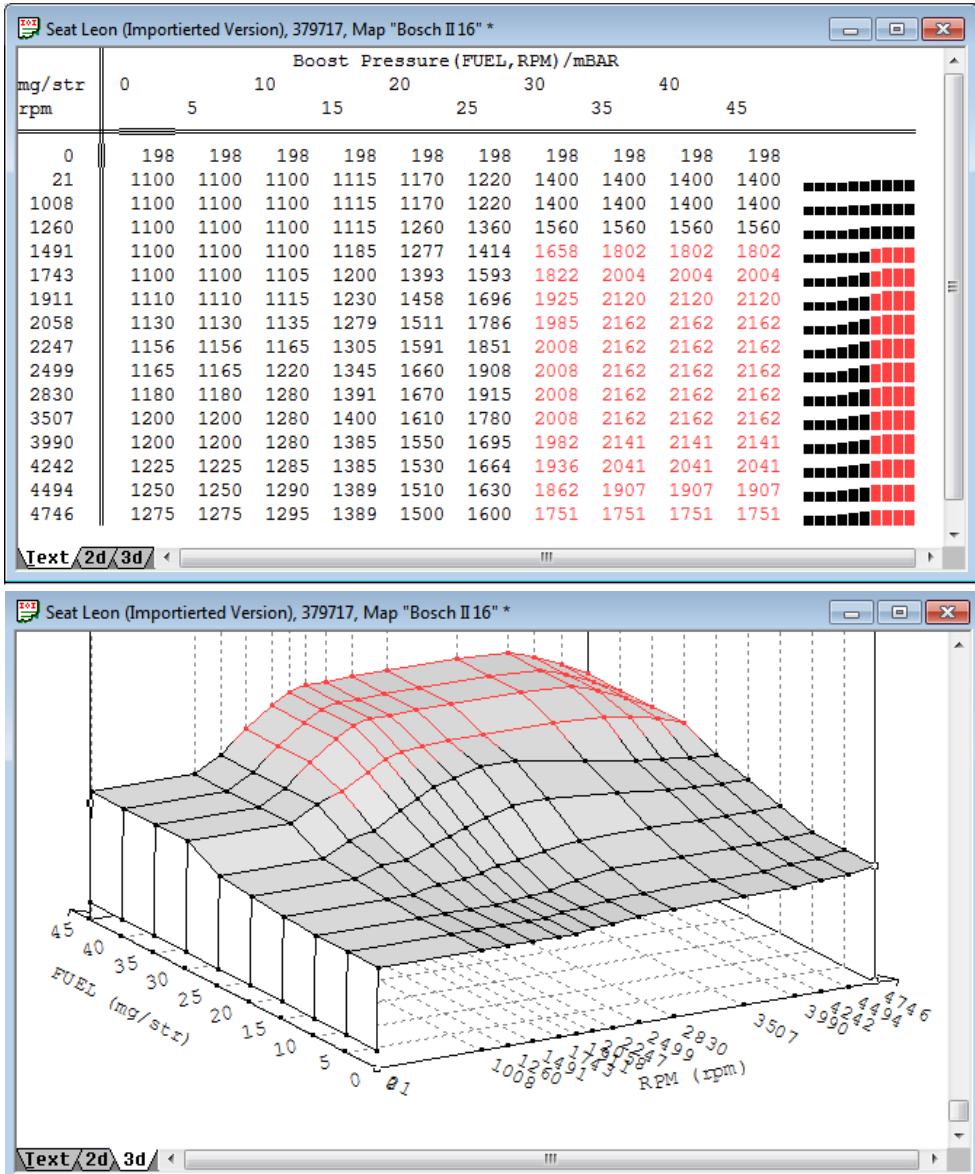


Figure 8: ECONOMY optimization – Intake Manifold Boost Pressure (Fuel, RPM/mBAR)

3 RESULTS

Analyzing the results for the engine's power output (Figures 9 and 10), the POWER/PERFORMANCE optimization led to a 36% increase in engine power (78 to 106 kW) while the ECONOMY optimization, which was aimed primarily at a decrease in fuel consumption and a climate-friendly improvement of the environmental map of the engine, maintained an increase in engine power of 23 % (78 to 96 kW). Both optimizations led to an increase in the power output, with room to improve the engine's fuel economy, or otherwise reduce fuel consumption. The POWER optimization led to a 9% decrease in fuel consumption (6.6 to 6.0 l/100 km) while the ECONOMY optimization, understandably led to an even larger, 13.5% decrease in fuel consumption (6.6 to 5.7 l/100 km).

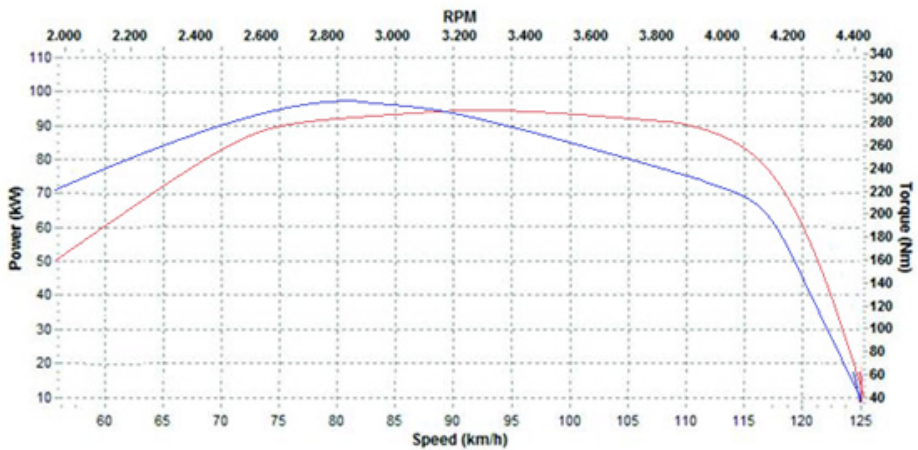


Figure 9: Power output following the ECONOMY optimization

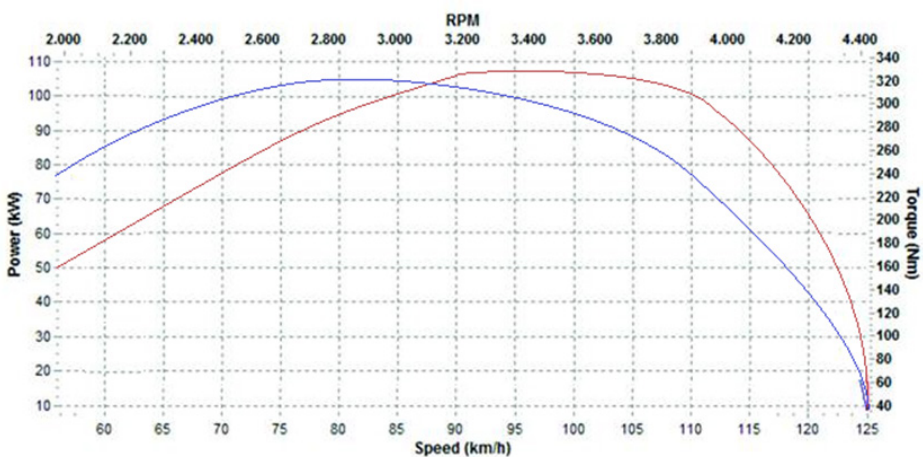


Figure 10: Power output following the POWER optimization



Figure 11: Fuel consumption – POWER optimization



Figure 12: Fuel consumption – ECONOMY optimization

The quantity of harmful exhaust components was measured following both optimizations. The results showed a major difference between the non-optimized engine and the same engine following the POWER, and especially the ECONOMY optimization (Figure 11, 12) regarding the CO₂ emissions. Due to the lowered fuel consumption, a more climate-friendly exhaust footprint from the 1.9 TDI engine was achieved as a direct consequence, and included a 42% decrease in CO₂ emissions (3.43% to 1.99% of the total volume of exhaust gases). Furthermore, even the POWER optimization led to a 30% reduction in CO₂ emissions (3.43% to 2.38% of the total volume of exhaust gases).

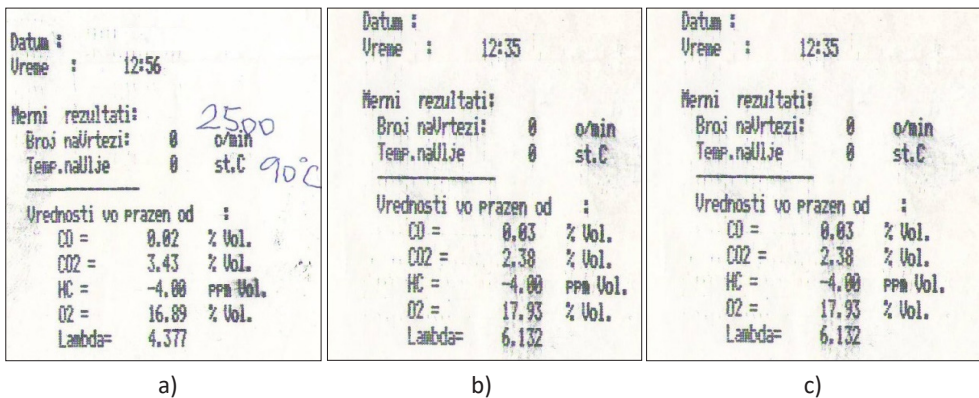


Figure 13: Exhaust emissions: a) Unoptimized; b) Economy; c) Power

4 DISCUSSION

The results show that the test-engine is designed to have a higher power output than what the factory control setting allows it. However, taking account of the market where the particular vehicle driven by this engine is being sold, the control maps chosen will reflect specific legal norms, such as environmental Standards, traffic safety norms, conditions for the technical approval of vehicles, taxation conditions, etc., in the countries that make the biggest part of the vehicle's market. The most attention is paid to the environmental norms, since they are controlled easily at the annual technical inspection of the vehicle, by measuring the quantity of harmful components in the vehicle's exhaust emission.

Both the POWER and ECONOMY optimizations are performed primarily by advancing the fuel injection timing. Immediately following the optimization, and according to the results, the engine demonstrates significantly better fuel economy, and, with it, a reduction in CO₂ emissions, but the advanced fuel timing will also inevitably lead to an increase in combustion temperature, which will lead to a rise in NOx emissions. Nevertheless, following both aftermarket optimizations, in the short-term the engine satisfies the required environmental norms in full, while the test-vehicle continues to meet the Euro 4 Emission Standards.

In theory, it is likely that long-term operation will lead to higher wear of certain components, but within the limits predicted by the manufacturer. The performed optimizations following prolonged operation, with great certainty, will lead to a more pronounced decrease in injection pressures and delayed fuel injection timing, which would increase the particulate matter (PM) emissions while decreasing NOx. It should be noted however, that engine emissions can be affected (sometimes significantly) even as the engine deteriorates due to normal wear and/or lack of proper service. This means that, even if the amount of NOx and PM in the exhaust emissions changes over time, the manufacturer predicted that it is highly unlikely that the vehicle's ecological standard will drop in the Euro 3 Standard.

It should be noted that gauging and evaluating the effect of the components' wear on the emissions quantity for engines with modern after treatment systems (Euro 5 and 6 Emission Standard) is considerably more complex, since these engines rely very heavily on the after treatment system to limit emissions, especially for NOx and PM.

5 CONCLUSION

The ongoing conflict in Ukraine and the current geopolitical state of the world have slowed down the economic recuperation following the COVID 19 pandemic significantly. This translates to a new economic crisis, and with-it rising fuel prices. Additionally, one of the positive consequences of the pandemic, the drop in CO₂ emissions in 2020 and 2021, is now on the rise as societies are getting back to their pre-COVID functioning. In response, the research conducted in preparation for this paper sought to analyze the implications of taking advantage of engine control and diesel engine aftermarket optimizations, which have the potential to minimize fuel consumption and reduce the GHG exhaust footprint of a diesel IC engine.

By performing a POWER and ECONOMY optimization on a sufficiently modern, 1.9 dm³, in-line, four-cylinder, four stroke, turbocharged direct injection engine, that complies with the Euro 4 Emission Standards, this paper proved that it is perfectly plausible to improve fuel economy, and, as a direct consequence, make the engine more climate friendly. At the same time, each of the optimizations maximized the power output of the engine, thereby meeting the operational needs of the engine and vehicle tested.

The major trade-offs for the environmental-engineering compromise are related to engine wear, which, in the short term, will be insignificant, but as this optimization required advancing the fuel injection timing, it will lead to an increase in local NOx emissions due to higher combustion temperatures. In the long term, as engine wear becomes more pronounced and results in decreased injection pressures and delayed fuel injection timing, the amount of PM emissions is likely to increase, while the NOx emissions will drop. It should be stressed that neither optimization will lead to larger engine wear than the one predicted by the manufacturer, or at

least not in the short-term, which, consequently, means that the test vehicle and engine will continue to meet the Euro 4 Emission Standards.

References

- [1] **F. Delasalle, D. Erdenesanaa:** *Planes, trains and (big) automobiles: How heavy transport can reduce emissions and save money*, World Resources Institute. 2019. Available: <https://www.wri.org/blog/2019/07/planes-trains-and-big-automobiles-how-heavy-transport-can-reduce-emissions-and-save>
- [2] **P. R. Teixeira et al.:** *MOVEIM v1.0: Development of a bottom-up motor vehicular emission inventories for the urban area of Manaus in central Amazon rainforest*, Geosci. Model Dev. Discuss. Volume 1-21. 2018. <https://doi.org/10.5194/gmd-2018-81>
- [3] **N. Hoofman:** A review of the European passenger car regulations – Real driving emissions vs local air quality, *Renew. Sust. Energ. Rev.*, Vol. 86, 2018
- [4] **W. A. Majewski, M. K. Khair:** *Diesel emissions and their control*, SAE Warrendale, Pennsylvania, USA. 2006
- [5] **C. M. Atkinson et al.:** *Model-based control of diesel engines for fuel efficiency optimization*. SAE. 2009. <https://doi.org/10.4271/2009-01-0727>
- [6] **R. Isermann:** *Engine modeling and control*, Springer Heidelberg, Berlin, Germany, 2014
- [7] **Z. Mirakovski:** *Optimization of the working parameters of an IC engine to reduce its fuel consumption and CO2 emissions*, Master Thesis, Faculty of Mechanical Engineering – Skopje, 2018
- [8] **G. A. Bell:** *Modern Engine Tuning*, Haynes Publishing, 1997
- [9] **Allied Market Research:** *Automotive Performance Tuning and Engine Remapping Services Market - Global Opportunity Analysis and Industry Forecast, 2021–2030*, 2023, Available: <https://www.alliedmarketresearch.com/automotive-performance-tuning-and-engine-remapping-services-market-A13880>
- [10] **J-Ball:** *ECM Tuning for Trucking/Transportation*, 2023, Available: <https://jballelectronics.com/industries/ecm-tuning-for-trucking-transportation/>
- [11] **J. Singh, C. Perisamy:** *Innovation in cohesive stock ECU Tuning And Turbocharging*, International Journal of Innovative Technology and Research, Vol. 4. p. 5252-5255, 2016.
- [12] **M. Nekoei, J. Koto, A. Priyanto:** *A Simple Fuzzy Logic Diagnosis System for Control of Internal Combustion Engines*, Jurnal Teknologi. Vol. 74, Iss. 5, p. p. 121-124, 2015. <https://doi.org/10.11113/jt.v74.4652>
- [13] **K. P. Wong, M. L. Tam, K. Li:** *Automotive engine power performance tuning under numerical and nominal data*, Control Engineering Practice, Vol. 20, p. P. 300-314, 2012

- [14] **X. Yu et al.:** *Internal combustion engine calibration using optimization algorithms*, Applied Energy. Vol. 305, 2022, 117894, <https://doi.org/10.1016/j.apenergy.2021.117894>
- [15] **UNECE:** *Road vehicle fleet at 31 December by vehicle category and age group*, UNECE Statistical Database, 2022
- [16] **Transport Community:** *Strategy for sustainable and smart mobility in the Western Balkans - Transport community treaty permanent secretariat's staff working document*, 2021
- [17] **Ministry of Interior:** *Rulebook for the technical inspection of vehicles*, Official Gazette of the Republic of North Macedonia 81/2010, 2010
- [18] **S. A. Ahmed et al.:** *Article Influence of Injection Timing on Performance and Exhaust Emission of CI Engine Fuelled with Butanol-Diesel Using a 1D GT-Power Model*, Processes, Vol. 7, Iss. 5, 299, 2019. <https://doi.org/10.3390/pr7050299>
- [19] **W. Tutak, A. Jamrozik, A. Bereczky:** *Effects of injection timing of diesel fuel on performance and emission of dual fuel diesel engine powered by diesel/E85 fuels*, Transport, Vol. 33, Iss. 3, p. 633-646, 2018. <https://doi.org/10.3846/transport.2018.1572>

ANALYSIS OF AGED CABLES` INSULATION WITH X-RAY FLUORESCENCE SPECTROMETRY

ANALIZA ELEKTRIČNE IZOLACIJE STARANIH KABLOV Z RENTGENSKO FLUOROSCENČNO SPEKTROMETRIJO

Nejc Friškovec^{1✉}, Manja Obreza¹, Marko Pirc², Klemen Sredenšek¹, Zdravko Praunseis¹

Keywords: cable ageing, polymer electrical insulation, x-ray fluorescence spectrometry, preventive maintenance, acceptance testing

Abstract

The paper provides an analysis with X-ray fluorescence spectrometry of aged cable samples. The work encompasses a review of the electrical, mechanical and chemical properties, as well as measurement methods for determining those parameters. The analyses are based on physical principles that allow us to assess the condition of the cable insulation. Using the physical properties and measurement results, mathematical models can be formulated to describe the ageing of individual materials in the presence of specific influences. The goal of the paper is to establish the foundation for the development of a measurement method using X-ray spectral analysis. The methodology assumes that the presence of specific elements decreases or increases on the material's surface as it ages. By using a standard indenter modulus test, we can determine reference points for X-ray spectral analysis. Sampling these points on differently degraded cables enables the establishment of criteria for acceptable cable insulation.

✉ Corresponding author: Nejc Friškovec, E-mail address: nejcfriskovec@hotmail.com

1 Faculty of Energy Technology, University of Maribor, Hočevarjev trg 1, Krško, Slovenia

2 Nuclear Power Plant (NEK), Vrbina 12, 8270 Krško, Slovenia

Povzetek

Delo zajema pregled električnih, mehanskih in kemijskih lastnosti ter merilnih metod za določanje njihovih parametrov. Analize temeljijo na fizikalnih osnovah, s pomočjo katerih lahko določamo stanje kabelske izolacije. S pomočjo fizikalnih lastnosti in merilnih rezultatov pa lahko oblikujemo tudi matematične modele, ki opisujejo staranje materialov ob prisotnosti posameznih vplivov. Cilj je zasnova podlage za oblikovanje merilne metode z rentgensko spektralno analizo. Metodologija temelji na predpostavki, da se s staranjem materiala na površju zmanjšuje oziroma povečuje prisotnost posameznih elementov. S pomočjo standardnega testa indenter modula lahko določimo referenčne točke, na podlagi katerih se izvede rentgenska spektralna analiza. Z vzorčenjem teh točk različno degradiranih kablov pa se vzpostavimo merila sprejemljivosti kabelske izolacije.

1 INTRODUCTION

The fundamental component of all systems utilising electrical energy is represented by electric cables. However, they are often overlooked and taken for granted. The primary purpose of conductors is to transmit electrical energy or information between components or devices. Conductors, typically cylindrical in shape, are surrounded by basic electrical insulation. Low and medium voltage cables, assuming polymer insulation, will be the focus of this paper. The conductors are categorised based on nominal voltage and current, determining their cross-section. Cables consist of one or more conductors, surrounded by a polymer sheath. Aging refers to the degradation of material and deterioration of the mechanical, electrical and chemical properties of electrical insulation, leading to cable destruction. External factors such as temperature, water presence, chemicals and UV light accelerate ageing. Thermal-oxidative degradation poses the greatest challenge, altering the material's structure and properties. Various non-destructive methods, including insulation resistance and dielectric loss measurements, are used to analyse insulation condition. Mechanical measurements, like tensile strength, and chemical analysis methods, such as thermogravimetric analysis, aid in assessing changes in the properties. Mathematical models or experimental data are relied upon to assess the remaining lifespan based on theoretical principles or data [1 - 5].

1.1 Polymer insulation

The electrical insulation separates conductive parts from each other electrically, meaning wires from each other and wires from the surroundings. The outer sheath, in addition to providing electrical protection, also offers mechanical protection to the conductors against environmental influences. An important role of electrical insulation is also to protect workers and users, as it shields them from direct contact and electric shock. Additionally, various colours of insulation facilitate easier orientation when connecting conductors to electrical components. Electrical insulation has standard electrical properties, which are categorised as follows [6]:

- volumetric resistance,
- surface resistance,
- insulation resistance,
- dielectric constant,
- dielectric losses, and
- dielectric strength.

In addition to the electrical properties of the insulation itself, the thermal, mechanical and chemical properties are also extremely important, as they influence the material's effectiveness and its ability to provide electrical insulation. The composition of the material itself determines whether the material can withstand prolonged exposure to various external influences. Essentially, we want materials to be resistant to the following factors [6]:

- fire,
- high temperatures,
- aggressive liquids,
- UV light,
- moisture, and
- to ionising radiation.

Various polymeric or other insulating materials are used, due to the need for optimal electrical and mechanical properties of electrical insulation. However, the electrical and mechanical properties change or deteriorate throughout the material's lifespan due to the ageing process. Material ageing depends on the material's production, maintenance, and, above all, the conditions under which it operates.

1.2 Electrical and mechanical properties

The mentioned electrical properties of the insulating material constitute an essential part of the conductor, as the essence of insulation lies in separating conductive parts from each other and reducing electrical losses. The most fundamental property of electrical insulation is its resistance. Measurements of IR are considered complex, since it is necessary to consider multiple factors.

In practice, the determination of IR is carried out using the "Megger" IR test, which is based on a non-destructive method. IR measurements are influenced by various factors, including temperature and humidity, making measurement conditions crucial. Periodic measurements allow for tracking trends and assessing insulation and electrical equipment conditions over time [7]. According to the IEC 60364-6 Standard, an installation cable must have at least 1 MΩ IR when measured, with a voltage of 500 V [8]. The relative dielectric constant describes the material's ability to behave like a capacitor, with values ranging between 2 and 3.5 depending on temperature and humidity [9]. Increases in capacitance and decreases in IR are explained by the concept of tangent delta or dielectric losses. Moisture ingress or partial immersion of insulation in water can increase capacitance and decrease IR, leading to the appearance of a real component of the current. The measurement of dielectric losses, known as $\tan\delta$, enables the detection of unnoticed cable conditions, such as local cable soaking or high humidity. Dielectric strength expresses a material's resistance to high voltage, determining the voltage it can withstand before breakdown occurs [10]. PDs, which can degrade the insulation, occur due to exceeding the dielectric strength limit of the surrounding material. PDs can be categorised into internal discharge, surface discharge and corona discharge [11]. Changes in mechanical properties, such as cable cross-section, maximum tensile strength, elongation at break, and hardness, reflect insulation and cable sheath ageing. The indenter method is used commonly for measuring degradation and mechanical properties, involving a small ball pressing against the cable to determine the indenter modulus [12].

1.3 Insulating materials and cable structure

The planning or selection of insulation depends primarily on the surroundings in which the cable will be located and the operating voltage. Depending on the complexity, the insulation material itself is also chosen accordingly. However, it should be noted that more resistant materials will fall into a higher price range. Cables using the sheath or insulation will be considered at a basic level:

- Poly vinyl chloride,
- Ethylene propylene rubber (EPR),
- Cross-linked polyethylene,
- Chloroprene or neoprene, and
- Chlorosulfonated polyethylene, or known commercially as Hypalon.

A typical structure of a basic cable is represented in Figure 1.

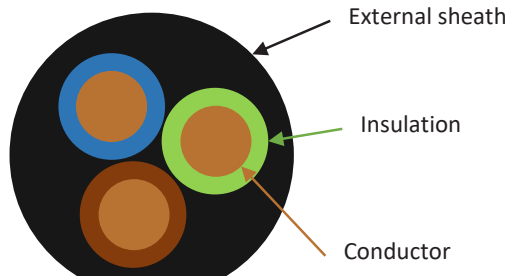


Figure 1: Cross-section of a cable with three conductors in insulation and a sheath

The cable used in our experiment consists of EPR used as the insulator and neoprene as the external sheath.

1.3.1 Ethylene propylene rubber

The ethylene-propylene rubber is a polymer chain manufactured through the reaction of ethylene and propylene. Both basic molecules are in a gaseous state at room temperature and atmospheric pressure. We obtain both molecules by splitting natural gas or petroleum [13]. The structures of the individual molecules are illustrated in Figure 2.

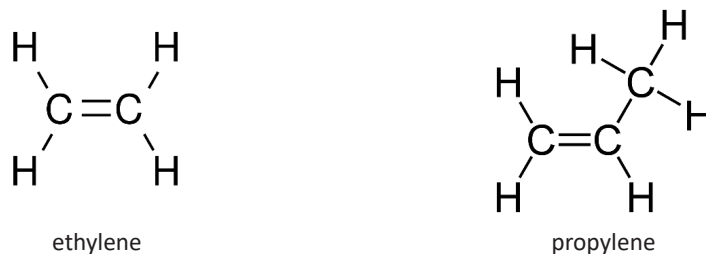


Figure 2: Chemical structure of ethylene and propylene [13]

The carbon (C) double bonds of both molecules can react with other molecules in various ways. Ethylene can bind with another ethylene or with propylene. Similarly, propylene can bind with another propylene or with ethylene. This forms a long chain of EPR. It is important to note that this chain is not two-dimensional, but three-dimensional, with the connection between molecules and their arrangement being random [13].

EPR is one of the most commonly used polymers for low and medium voltage cables. As mentioned, the basic components include ethylene and propylene, and additional components such as hexane, diene and a catalyst solution are also classified as basic ingredients. All these components must be extremely pure and dry for the manufacturing process. The amorphous EPR itself has very poor mechanical properties, so special additives need to be introduced to improve both its mechanical and electrical characteristics [14].

Materials such as clays, talc, fillers, silica, aluminium oxide, and other minerals, are added to the base EPR mixture to produce electrical insulation. In addition to these primary additives, other additives, such as metal oxides, plasticisers, antioxidants, zinc oxide, lead oxide, and other substances, are introduced into the mixture to optimise the manufacturing process.

Since EPR is fully saturated and nonpolar, this polymer exhibits excellent resistance to ozone, oxidation, high temperatures, water and polar solvents. EPR with a lower percentage of ethylene is amorphous and easier to process, while EPR with a higher percentage of ethylene demonstrates better mechanical properties. The resistance of EPR to all the beforementioned factors, as well as its resistance to corona, formation of water trees and other mechanical stresses, presents a significant advantage, and is a reason for the frequent use of this polymer as electrical insulation. As mentioned earlier, more than 10 different additives are introduced to EPR. Additionally, paraffinic, and naphthenic oils are added to the mixture as plasticisers and for optimising the extrusion process [15].

1.3.2 Neoprene

Chloroprene, also known as neoprene, is an emulsion polymer composed of 2-chlorobut-1,3-diene. Due to the presence of chlorine, neoprene is polar, which is reflected in its exceptional mechanical properties, such as tensile strength, elasticity, resistance to weathering, chemicals, oils and fire. In addition to improved mechanical properties, neoprene also exhibits good electrical properties, making it a popular material for cable insulation. Neoprene is also used frequently for cable sheaths [16].

As the temperature increases, the IR of neoprene decreases, a result of ion movement and the transition of neoprene from the crystalline phase to the amorphous phase. During this transition, the ions in the neoprene create dipoles, leading to increased conductivity. This phenomenon stems from the breaking of C-Cl bonds, causing the release of chlorine ions. These ions then react with ZnO, resulting in an increased concentration of impurities such as $ZnCl_2$ in the neoprene. This, in turn, causes increased electrical conductivity [17]. In addition to this reaction, chlorine also reacts with lead, forming $PbCl_2$, although these molecules are less problematic. $ZnCl_2$ is particularly challenging, as it is soluble in water, potentially causing corrosion of the surrounding materials [18]. Table 1 provides typical values for the electrical and mechanical properties of neoprene and EPR used in electrical insulation or sheathing.

Table 1: Characteristics of insulation material based on neoprene [19, 20]

Characteristics		Neoprene	EPR
Maximum operating temperature [°C]	Normal	90	40
	Maximum	130	120
	Short-term	250	180
Tensile strength [kg/mm ²]		2,8	0,95
Maximum elongation [%]		600	250-550
Specific resistance [Ωcm]		10 ¹¹	10 ¹⁵ -10 ¹⁷
Dielectric constant [1kHz]		9	3,17-3,34
Dielectric strength [kV/mm]		19,7-27,6	35,4

2. METHODOLOGY

The term "ageing" denotes the inevitable degradation of electrical and mechanical properties, accompanied by chemical structural changes in materials, polymers, or cable insulation, leading ultimately to their dysfunction or failure. Ageing in polymeric materials is an inherent process affecting all plastic materials. As cables age, both the electrical and mechanical properties of the constituent materials deteriorate, resulting in increased material brittleness and vulnerability to external factors. Chemical changes in polymers, such as alterations in the glass transition temperature, crystallisation, and melting, intensify with ageing, necessitating laboratory analyses for detection. X-ray Fluorescence Analysis (XRF) is a rapid, precise and non-destructive analytical method used for determining the chemical composition of materials, applicable across various industries, including metallurgy, cement, petroleum, polymers, food, geology and mining. XRF, which can detect elements ranging from beryllium to uranium, operates in energy-dispersive and wavelength-dispersive modes, with a focus on energy dispersion here. This method's accuracy and reliability make it suitable for analysing both standard and non-standard samples, enabling the identification of ageing-related changes such as the reduction of elements like chlorine and barium in aged cables, facilitating the establishment of acceptance criteria [21-24].

2.1 Theoretical background of XRF

X-ray beam or X-ray can be perceived as electromagnetic radiation, or as a photon with a specific energy. For easier understanding, we will describe it as a high-energy form of electromagnetic radiation with a wavelength between 10 picometers and 10 nanometers.

The spectrum of X-rays and other electromagnetic radiation with specified wavelength and corresponding energy is shown in Figure 3.

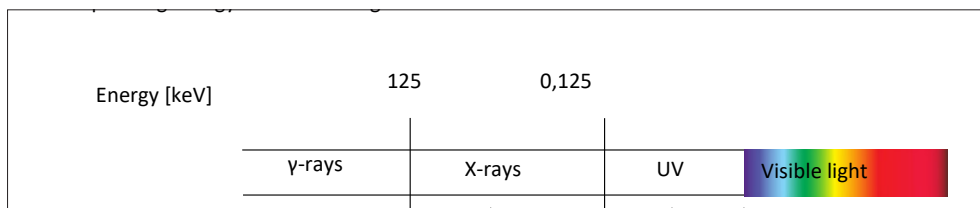


Figure 3: Spectrum of electromagnetic radiation

X-rays are generated through the conversion of kinetic energy acquired by an electron during acceleration with high voltage into electromagnetic radiation due to collisions and interactions [23]. To produce X-rays, a generator and electrodes are utilised, where the X-ray tube furnishes the requisite environment and electrons, while the generator provides the electrical voltage to electrodes. Matter interacts with X-rays through fluorescence, Compton scattering and Rayleigh scattering, with X-ray energy absorption contingent on the material's thickness, density, composition and the energy of the X-ray itself. The atom's classical model comprises a nucleus containing positively charged protons and neutrally charged neutrons, encircled by an electronic shell housing negatively charged electrons arranged in orbitals [25]. Electron ejection occurs when an atom is impacted by an X-ray beam with greater energy than the binding energy of the electron, leading to radiation absorption and fluorescence intensity. X-ray spectrometry determines element concentration quantitatively, employing empirical calculations or sophisticated theoretical methods, along with standard reference samples for accuracy [26].

2.2 Analysis of an aged sheath and insulation of a cable sample

The portable X-ray spectrometer NITON XL3T 980 GOLD++ was utilised for the sample analysis. The analyser was equipped with a large geometrically optimised silicon detector and an X-ray tube of 50 keV. The adjustment of sample thickness can be made using the analyser software, which is always crucial in polymer analysis. Polymers are composed of lightweight materials, allowing deep penetration of X-rays into them. Easy sample analysis is facilitated by the software, as not only the energy at which responses occur are displayed, but also the corresponding elements. Figure 4 shows the analyser performing sample measurements.



Figure 4: Analyser NITON XL3T 980 GOLD++

The sample under analysis is a cable previously used in a lighting installation exposed to high temperatures exceeding 45 °C, locally even higher. The healthy section of the cable experienced temperatures ranging from 40 to 50 °C, while the partially degraded section endured temperatures between 55 and 65 °C. The completely degraded portion was subjected to temperatures ranging from 75 to 85 °C. Moreover, the environment also exhibited high humidity, persisting for 40 years. IR measurements were conducted on all sections, to establish a reference for the electrical insulation and sheath condition. The cable comprises a neoprene sheath and EPR insulation, with an unknown material filler between them. Given the cable's exposure to

a dusty environment, potential impurities need identification and removal. The initial analysis involves IR measurements on all sections, including the sheath and conductors. The indentation modulus will gauge the electrical insulation condition and aid in interpreting the X-ray spectral analysis results.

Figure 5 shows the most degraded section of the cable sample.



Figure 5: Part of the degraded cable sample

3. RESULTS

3.1 IM measurements

The IM measurements were taken as a reference on individual sections of the cable. The condition of the cable was divided into three parts: healthy (soft), partially damaged (medium), and damaged (hard) cable. The IM-sheath measurements were conducted on all three sections of the cable, and XRF measurements were also performed on all three parts. Table 2 shows the sheath measurements with the indentation modules.

Table 2: The sheath measurements with the indentation modulus

	Healthy (soft) sheath of cable IM [N/mm]	Partially damaged (medium) sheath of cable IM [N/mm]	Damaged (hard) sheath of cable IM [N/mm]
Average	13,5	66,2	193,7
Standard Deviation	0,9	50,1	38,6

From the average value and Standard Deviation of the measurements shown in Table 2, significant deviations were observed in a very small section of the cable, indicating varying degrees of sheath degradation relative to the extent and length of the cable.

IM measurements were conducted on the degraded sections of insulation, specifically on all three wires: yellow-green, blue, and brown. Table 3 displays the IM values on the individual sections of the brown insulation.

Table 3: The insulation measurements with the indentation modulus

	Healthy (soft) sheath of cable IM [N/mm]	Partially damaged (medium) sheath of cable IM [N/mm]	Damaged (hard) sheath of cable IM [N/mm]
Average	11,5	17,8	24,9
Standard Deviation	1,2	4,2	9,9

The measurements revealed the greatest degradation on the brown wire, while no significant signs of degradation were observed on the other wires. Consequently, the most detailed analysis was performed on the brown insulation.

In this case, the Standard Deviation was much smaller than that of the sheath measurement. However, for more precise results, the highest and lowest points were disregarded. It should be emphasised that, due to the non-critical state of IM in the insulation, it was smaller than in the sheath.

3.2 XRF measurements

The results of the jacket measurements are shown in Figure 6.

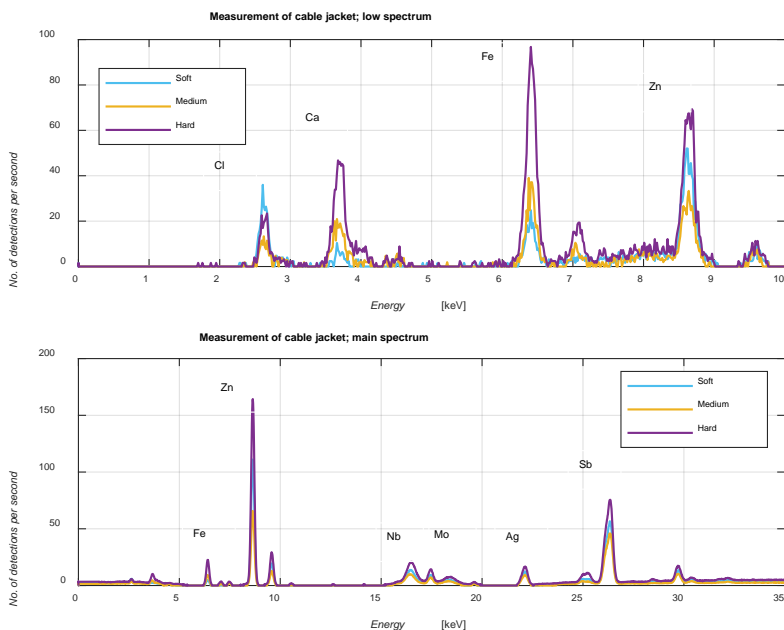


Figure 6: The results of the sheath measurements with XRF

The measurements in Figure 6 indicate that the presence of chlorine generally decreases with ageing, which could be attributed to the degradation of the crystal structure, especially the covalent bonds of chlorine in the neoprene. An increase in calcium value with ageing was

observed, suggesting potential leaching from the interior, as a higher presence of calcium was detected in the healthy section of the cable during the filler measurement. Higher iron values were recorded in the more degraded sample, possibly indicating contamination or leaching from the interior, a scenario applicable to zinc as well. The presence of zinc in cable insulation is expected, as it is added to the polymer to improve the mechanical properties in the form of zinc ions. It should be noted that the sheath remains on the cable, allowing the possibility of X-ray penetration depth measuring filler and insulation. Based on this assumption, measurements were conducted where individual parts were removed and measured separately. The results of the jacket measurements from the outside of the cable are presented in Figure 7.

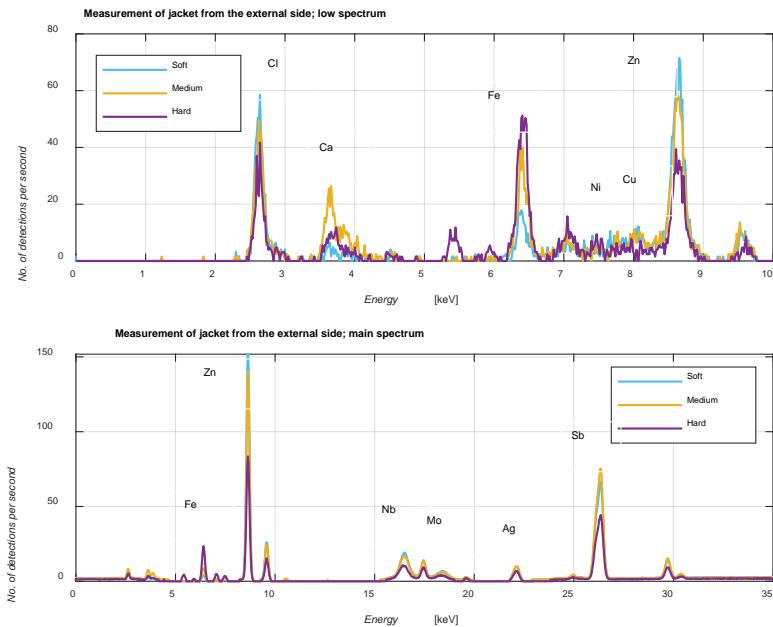


Figure 7: The results of the jacket measurements from the removed cable’s exterior with XRF

Similar trends as those observed in the cable measurements emerged in these measurements (Figure 7). With the ageing of the cable, the presence of chlorine decreases, while the presence of iron increases. However, zinc presence decreased in this case, contrary to when the insulation was still on the cable. This difference in results could be attributed to different measurement points, contamination, or indicates that zinc may be present in the filler or insulation.

Additionally, the measurements detected the presence of nickel and copper, with the concentration of copper decreasing with ageing, suggesting contamination. The presence of these two materials generally indicates contamination. In the main spectrum, niobium and molybdenum showed a decreasing trend with ageing. Similarly, antimony exhibited such a trend, with slight deviations observed in the moderately aged sample.

The results of sheath measurements from the inside are depicted in Figure 8.

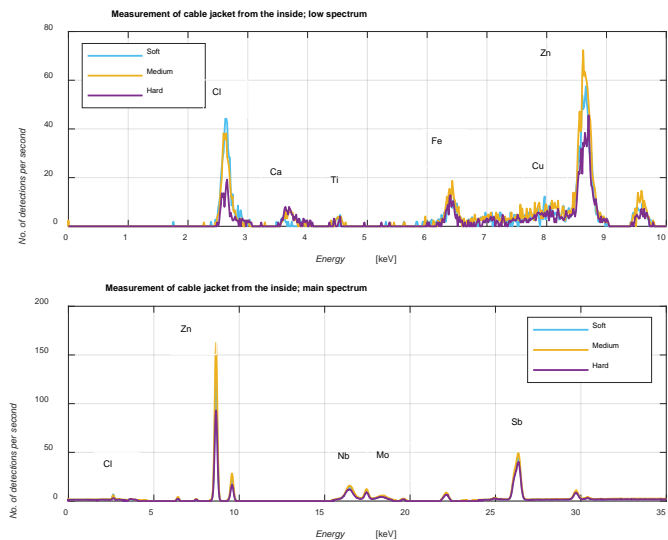


Figure 8: The results of sheath measurements from the inside of the cable

Figure 8 presents a pronounced decrease in chlorine concentration.

Iron and zinc maintained a decreasing concentration trend with ageing. No clear trend was observed for other elements, as measurements from the moderately healthy sheath deviated. This deviation may be attributed to contamination of the inner sheath due to the filler.

Figure 9 shows the results of filler measurements from all three parts of the cable.

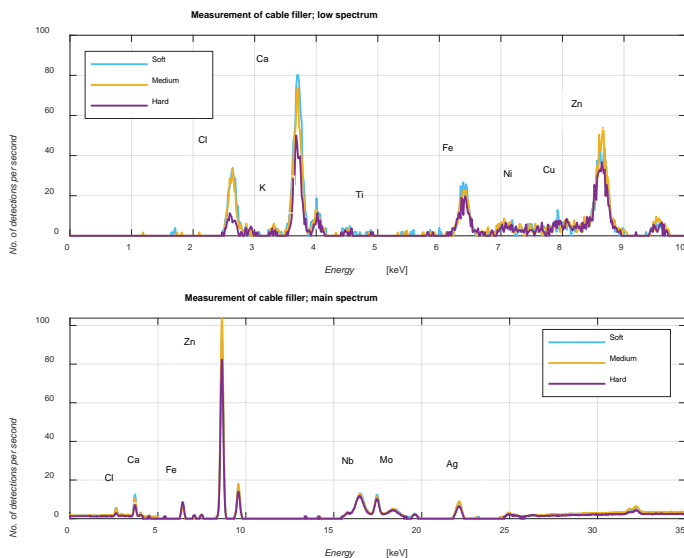


Figure 9: The results of the filler measurements

From the results presented in Figure 9, a trend of decreasing chlorine concentration with ageing is evident, which also applies to the filler. The most pronounced decrease was observed in the calcium. The presence of calcium may indicate the use of clay as an additive in the polymer, hence, monitoring this element is acceptable. Similar trends to those observed in other measurements were also noticeable for iron and zinc. The measurements also revealed concentrations of potassium, titanium, nickel and copper. The main spectrum measurements indicated decreasing trends for niobium, molybdenum and antimony.

The measurements of the cable insulation, specifically the brown-coloured insulation, which exhibited the greatest deviation in IM, are shown in Figure 10.

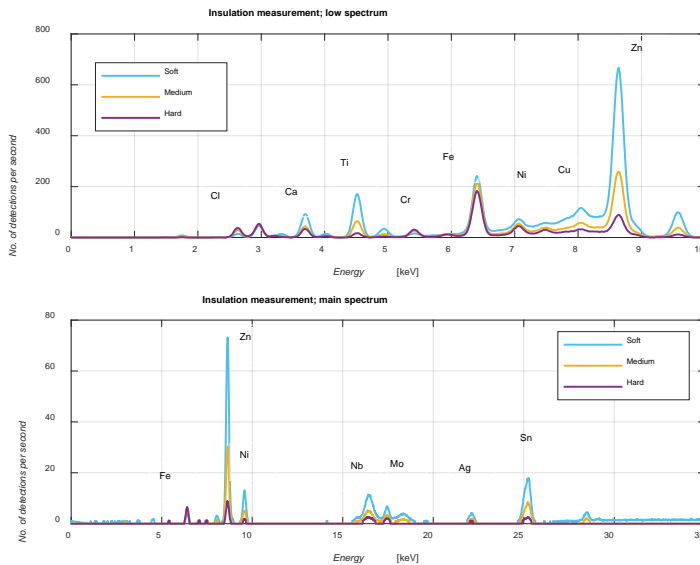


Figure 10: The results of the measurements on the brown-coloured insulation

In the low-spectrum measurements, the presence of chlorine, calcium, titanium, chromium, iron, nickel and copper reappeared, as shown in Figure 10. Calcium and nickel are elements present in the EPR itself. However, the measurements showed a decreasing concentration trend with ageing. Additionally, a decrease in zinc was observed, which is added to the EPR as a zinc oxide binder. The main spectrum measurements exhibited pronounced trends in niobium, molybdenum and antimony, where the concentrations decreased significantly with ageing.

Table 4 displays the proportion of individual elements in the healthy, partially healthy, and degraded samples.

Table 4: The proportion of elements in cable samples of the insulation

Element	Proportion of elements in the healthy sample [ppm]	Proportion of elements in the partially healthy sample [ppm]	Proportion of elements in the degraded sample [ppm]
Chlorine	2954,79	7973,02	23321,85
Chromium	58,76	326,63	941,11
Nickel	23,12	164,97	638,58
Tungsten	66,07	59,69	44,53

The results in Table 4 indicate a trend of decline or increase. The increase in concentration sometimes occurs due to the precipitation of this element on the surface.

4 DISCUSSION

Cables are crucial for integrating renewable sources into the power grid and ensuring smooth operation across all energy system stages. They play a vital role in critical infrastructures like nuclear power plants, ensuring uninterrupted safety system operation. Preventive maintenance is essential for early fault detection. Various methods, including mechanical and chemical property assessments, are used for cable maintenance and condition assessment. Efforts to simplify and standardise assessment methods involve establishing acceptability criteria. X-ray spectral analysis monitors the concentration trends of elements in cable sheaths and insulation during ageing, aiding in issue identification.

In addition to understanding chemical composition, considering Standard measurements with known acceptability criteria that determine cable condition is crucial. Trends of decreasing or increasing element concentrations are determined by performing IR measurements and XRF measurements on individual cable sections. Decreasing chlorine concentration in the sheath indicates the breakdown of covalent bonds in the crystal structure of the neoprene, indicating the ageing of this material. The presence of calcium in the filler suggests the use of clay in the polymer itself, while the decreasing trend in its concentration indicates material precipitation with ageing. In the cable insulation, a significant decreasing trend in antimony concentration was observed, which is used in polymers to add flexibility and fire resistance.

It is important to note that there is no universal method for assessing cable condition, as cable insulation consists of various materials with different properties. However, employing multiple methods can provide a comprehensive picture. This thesis serves as a foundation for further research and the potential application of X-ray spectral analysis, which is a useful method for monitoring the condition of cable electrical insulation.

References

- [1] **S. Ilie, R. Setnescu, E. M. Lungulescu, V. Marinescu, D. Ilie, T. Setnescu, G. Mareş:** *Investigations of a mechanically failed cable insulation used in indoor conditions*, Polymer Testing, let. 30, No. 2, p.p. 173–182, 2011
- [2] **E. Mustafa, R. S. A. Afia, Z. Á. Tamus:** *Condition Monitoring Uncertainties and Thermal-Radiation Multistress Accelerated Aging Tests for Nuclear Power Plant Cables: A Review*, Periodica polytechnica electrical engineering and computer science, No. 1, p.p. 20–32, 2020
- [3] **J. - L. Parpal, J. - P. Crine, C. Dang:** *Electrical aging of extruded dielectric cables*, A physical model, IEEE Transactions on Dielectrics and Electrical Insulation, No. 2, p.p. 197–209, April 1997
- [4] **J. Li, et al.:** *The effect of self-producing heat and external radiation on the insulating property of wire*, Procedia Engineering, No. 135, p.p. 151–159, 2016
- [5] **M. H. Shwehdi, M. A. Morsy, A. Abugurain:** *Thermal aging tests on XLPE and PVC cable insulation materials of Saudi Arabia*, 2003 Annual Report Conference on Electrical Insulation and Dielectric Phenomena, p.p. 176–180, 2003
- [6] **M. Pecht, R. Agarwal, F. P. McCluskey, T. J. Dishonghm S. Javadpour, R. Mahajan:** *Electronic packaging materials and their properties*, ZDA: CPC press LLC, 1999
- [7] **Megger:** *The complete huide to electrical insulation testing*, 2006
- [8] **IEC 60364:** *Priporočila za meritve električnih inštalacij (IEC 60364-6)*, 2005
- [9] **H. Torkaman, F. Karimi:** *Measurement variations of insulation resistance/polarization index during utilizing time in HV electrical machines*, A survey, Measurement, No. 59, p.p. 21–29, 2015
- [10] **G. Faria, M. Pereira, G. Lopes, J. Villibor, P. Tavares and I. Faria:** *Evaluation of Capacitance and Dielectric Dissipation Factor of Distribution Transformers*, Experimental Results, 2018 IEEE Electrical Insulation Conference (EIC), ZDA, pp. 336–339, 2018
- [11] **W. J. K. Raymond, H. A. Illias, A. H. A. Bakar, H. Mokhlis:** *Partial discharge classifications: Review of recent progress*, Measurement, p.p. 164–181, 2015
- [12] **K. L. Simmons, A. F. Pardini, L. S. Fifield, J. E. Tedeschi, M. P. Westman, A. M. Jones, P. Ramuhalli:** *Determining remaining useful life of aging cables in nuclear power plant interim study FY13*, U.S department of energy, ZDA, september 2013.
- [13] **R. J. Arhart:** *The chemistry of ethylene propylene insulation I*, IEEE Electrical Insulation Magazine, No. 5, p.p. 31–34, 1993
- [14] **R. J. Arhart:** *The chemistry of ethylene propylene insulation II*, IEEE Electrical Insulation Magazine, No. 6, p.p. 11–14, 1993
- [15] **A. K. Sen:** *Cable technology*, Rubber Products Manufacturing Technology, A. K. Bhowmick (ur.), M. M. Hall (ur.), and H. A. Benewey (ur.). New York, 1994
- [16] **Handbook of elastomers:** 2. edition, ZDA: CRC Press, 2001

- [17] **B. P. Kapgate, C. Das:** *Electronic applications of chloroprene rubber and its composites, Flexible and Stretchable Electronic Composites*, p.p. 279–304, 2016
- [18] **F. J. Boerio, S. G. Hong:** *Degradation of rubber-to-metal bonds during simulated cathodic delamination*, The Journal of Adhesion, No. 1–4, p.p. 119–134, 1989
- [19] **R. J. Schaefer:** *Mechanical properties of rubber*, v *Harris' Shock and Vibration Handbook*, 6. edition, A. Piersol (ur.), T. Paez (ur.), McGraw-Hill Companies Inc, 2010, p.p. 33.1–33.18
- [20] **G. Akovali:** *Plastic materials: chlorinated polyethylene (CPE), chlorinated polyvinylchloride (CPVC), chlorosulfonated polyethylene (CSPE) and polychloroprene rubber (CR)*, Toxicity of building materials, p.p. 54–75. Woodhead Publishing, 2012
- [21] **G.E Sliter:** *Overview of research on nuclear plant cable aging and life extension, SMIRT-12*, p.p. 199–2003, 1993
- [22] **M. Pirc, J. Avsec, N. Č. Korošin, U. L. Štangar, R. C. Korošec:** *Cable aging monitoring with differential scanning calorimetry (DSC) in nuclear power plants*, Transactions of FAMENA, p.p. 87–98, 2018
- [23] **G. N. Dolenko, O. K. Poleshchuk, J. N. Latosińska:** X-ray emission spectroscopy, methods, Encyclopedia of spectroscopy and spectrometry, p.p. 2984–2988, 2010
- [24] **B. Beckhoff, B. Kanngießer, N. Langhoff, R. Wedell,** *Handbook of Practical X-Ray Fluorescence Analysis*, 2006
- [25] **O. M. H. Ahmed, et al.:** *Quality assessment statistic evaluation of X-ray fluorescence via NIST and IAEA standard reference materials*, World Journal of Nuclear Science and Technology 7.2, p.p. 121–128, 2017
- [26] **R. Sitko, B. Zawisza:** *Quantification in X-Ray Fluorescence Spectrometry*, X-ray spectroscopy, p.p. 137–162, 2012

Nomenclature

(Symbols)	(Symbol meaning)
UV	Ultraviolet
IM	Indenter module
tan δ	Dielectric losses
VLF	Very low frequency
Un	Nominal voltage
PD	Partial discharges
IAEA	International Atomic Energy Agency
EPR	Ethylene propylene rubber
IEC	International Electrotechnical Commission
XRF	X-ray fluorescence spectrometry
IR	Insulation resistance

CONCEPTUAL TECHNO-ECONOMIC ANALYSIS OF RETROFITTING A 210 MW THERMAL HEAVY-OIL POWER PLANT WITH A MOLTEN SALT THERMAL ENERGY STORAGE SYSTEM FOR RENEWABLE POWER: A CASE ANALYSIS OF TEC NEGOTINO

KONCEPTUALNA TEHNO-EKONOMSKA ANALIZA OPREME 210 MW TERMALNE ELEKTRARNE NA TEŽKO OLJE S SISTEMOM ZA SHRANJEVANJE TERMALNE ENERGIJE S POMOČJO STALJENE SOLI ZA OBNOVLJIVE ENERGIJE: ANALIZA PRIMERA TEC NEGOTINO

Dragan Minovski¹, Marija Sterjova[✉]

Keywords: retrofitting, MSTES system, electric salt heater, decarbonization, grid flexibility, analysis variants cases, techno-economic assumptions

Abstract

This study conducts a conceptual techno-economic analysis to explore the possibility of retrofitting a 210 MW thermal heavy-oil power plant, TEC Negotino, with a molten salt thermal energy storage system (a Carnot battery). The proposed approach enables storage of surplus or

[✉] Corresponding author: Master's degree student Marija Sterjova, Goce Delcev University, Faculty of Electrical Engineering, Krste Misirkov 10-A, 2000 Stip, North Macedonia, Tel.: +389 32 550 000, E-mail address: marija.22512@student.ugd.edu.mk

¹ Goce Delcev University, Faculty of Electrical Engineering, Krste Misirkov 10-A, 2000 Stip, North Macedonia

curtailed renewable electricity on the grid in the form of thermal energy. This initial exploration involves analysing the sensitivity of annual energy yield, load factor, total investment cost, annual O&M cost and levelized cost of a discharging electricity with varying discharging duration, thermal storage capacity and charging duration. The results demonstrate that the most favorable annual roundtrip efficiencies and lowest levelized cost of discharge electricity were obtained for longer discharge duration (in full load hours). This approach of the possibility of repurposing TEC Negotino not only prioritizes the potential for the comprehensive decarbonization of the thermal power plant, but also conserving the majority of jobs within the power plant, making it a sustainable and economically viable initiative.

Povzetek

Ta študija izvaja konceptualno tehnično-ekonomsko analizo za raziskovanje možnosti naknadnega opremljanja 210 MW termoelektrarne na težko olje, TEC Negotino, s sistemom za shranjevanje toplotne energije iz staljene soli (Carnotova baterija). Predlagani pristop omogoča shranjevanje presežne ali okrnjene obnovljive električne energije v omrežju v obliki toplotne energije. To začetno raziskovanje vključuje analizo občutljivosti letnega donosa energije, faktorja obremenitve, skupnih naložbenih stroškov, letnih stroškov O&M in izravnanih stroškov odvajanja električne energije z različnim trajanjem praznjenja, kapaciteto toplotnega shranjevanja in trajanjem polnjenja. Rezultati kažejo, da so bili najugodnejši letni povratni izkoristki in najnižji izravnani stroški električne energije za praznjenje doseženi pri daljšem trajanju praznjenja (v urah polne obremenitve). Ta pristop možnosti ponovne namembnosti TEC Negotino ne daje prednosti le potencialu celovite dekarbonizacije termoelektrarne, temveč tudi ohranjanju večine delovnih mest v elektrarni, zaradi česar je to trajnostna in ekonomsko uspešna pobuda.

1 INTRODUCTION

In the pursuit of cost-effective and strategically aligned energy transition, this paper proposes repurposing a conventional fossil fuel power plant through the integration of a utility-scale molten salt thermal energy storage (MSTES) system, known as the large Carnot battery [1]. This transformative approach not only extends the life of fossil fuel plants (giving them a second green life), but also contributes to the green economy and grid flexibility [11] (effectively smoothing out fluctuations from both renewable energy demand and supply, contributing to a sustainable and resilient energy infrastructure). Following in-depth studies [5]-[7] and exploring the potential of repurposing fossil fuel power plants, including Chile's example of a coal plant retrofit with molten salt storage [8], we spotlight TEC Negotino, a 210 MW fossil fuel power plant on the brink of a remarkable transformation.

As a background research, section 2 delves into the expanded applications of MSTES systems for repurposing conventional fossil fuel plants, extending beyond concentrated solar power (CSP) systems to encompass Power-to-Heat (P2H) strategies with renewable energy (solar photovoltaic (PV) and wind power) [5]. This section explores practical examples and initiatives, such as Germany's commitment to repurposing decommissioned coal plants for substantial thermal storage facilities [4]. In section 3, we focus on a conceptual techno-economic analysis (based on assumptions), evaluating the performance and cost of retrofitting the existing conventional power plant TEC Negotino with the integration of MSTES. This involves the incorporation of an

electric salt resistance heater (ERH), thermal storage system and a molten salt steam generator. The analysis examines the sensitivity of annual energy yield, load factor, total investment cost, annual operation and maintenance (O&M) cost, and the levelized cost of discharging electricity with varying the discharging duration, thermal storage capacity and charging duration. In section 4, the Conclusion provides a concise recap of the main results and outcomes of the conceptual analysis on the possibility of retrofitting TEC Negotino with a MSTES system. Additionally, it suggests further recommendations with the next steps in the research.

2 BACKGROUND

During the last decade, a promising solution that has gained traction in recent years is retrofitting fossil fuel plants with CSP and MSTES systems [2], [3]. To expand the application of MSTES from its commercial use with CSP technologies to other renewable energy (RE) technologies such as solar PV and wind turbine plants, the following concepts are being prepared for market implementation [5]:

- Surplus, or curtailed variable RE electricity available in the grid from PV and wind power plants, can be stored as thermal energy (P2H) using electric molten salt heaters during the charging mode of a MSTES system. Subsequently, at discharge, the stored heat is converted back to power (Heat-to-Power - H2P) through a Rankine cycle. Fig. 1 provides a schematic representation of this concept, serving as the initial reference for ongoing analysis throughout the paper.
- Renewable power can be transformed into heat (P2H) through the use of high-temperature heat pumps for charging a MSTES system. Subsequently, during discharge, the stored heat is converted back into power (H2P) through a closed air Brayton cycle.

Fig. 1 illustrates the integration of a high-temperature MSTES system with ERH, thermal energy storage (hot and cold molten salt tank) and molten salt steam generator, to store and convert heat into power when needed [8], [9].

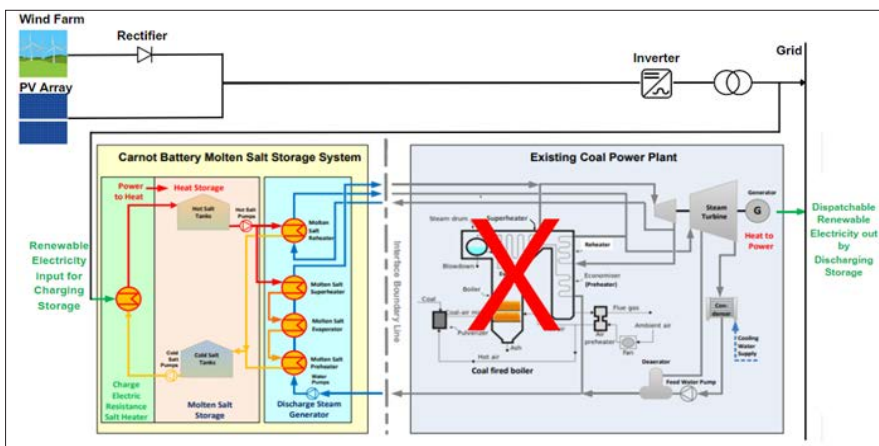


Figure 1: Schematic illustration of the integration of a high-temperature MSTES system into an existing coal plant, making use of its existing Rankine steam cycle

As we can see from Fig. 1, when the power output from both wind and PV systems exceeds the power grid's demand, the surplus electricity is converted into thermal energy by the electric heater and stored in storage system (during the charging cycle shown in Fig. 2). If the power demand exceeds renewable capacity, a steam turbine is activated, utilizing stored heat from the hot tank to generate power (using the existing Rankine steam cycle). Hot molten salt, initially stored in the hot tank, is then pumped to the cold tank, releasing thermal energy which can be used to generate steam for a steam turbine to produce electricity (during the discharging cycle shown in Fig. 2). The process of delivering the stored energy back to the grid is using the former fossil fuel plant's existing infrastructure (power blocks and grid connections). After transferring the hot molten salt to the cold tank, it is then ready to be recharged with thermal energy and the process can begin again. Optional backup co-firing can be used if storage reaches a critical level and cannot provide sufficient energy. The research assumes that the conventional heavy-oil fuel boiler in the case of TEC Negotino is not operational.

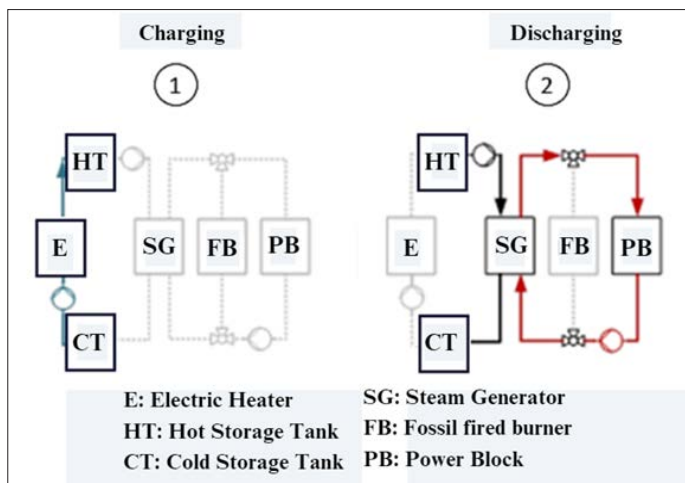


Figure 2: Operating modes of the MSTES of a model without the optional inclusion of fossil fuel boilers [6]

Fig. 3 illustrates examples of typical molten salt heated steam generator systems, including the 6,6 MWe molten salt heaters used at the SQM Nitrate Plant located in Coya Sur, Chile.

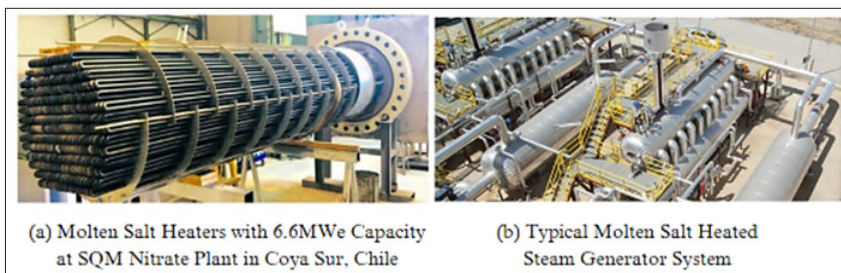


Figure 3: Illustration of a (a) molten salt resistance heaters for charging, and (b) a molten salt heated steam generator [5], [7]

Currently, molten salt, also known as "Solar Salt", a binary mixture of sodium nitrate (60 wt%) and potassium nitrate (40 wt%); (60 wt% NaNO₃ - 40 wt% KNO₃), appears as an efficient and durable energy storage salt composition for MSTES system retrofit applications, due to its high heat capacity, non-flammable and non-toxic properties, and longevity of over 30 years without degradation [7]. Solar Salt has a maximum temperature limit of 565°C, which demonstrates the capability to provide superheated steam up to 550 °C for power generation [2], [5]- [7], [10].

In 2018, the official German government coalition program [4] incorporated the concept of transforming decommissioned coal plants into thermal storage facilities. The program commits the German coalition government to "examine the extent to which power plant sites no longer needed in future may be used for large thermal storage plants" (lines 3321-3322). The German Aerospace Center (DLR) has played a pivotal role in exploring the technical and economic feasibility of incorporating solar technologies and molten salt storage into coal-fired power plants. The successful implementation of concentrated solar power and thermal energy storage technology can be seen in the 110 MW Cerro Dominador CSP project in Chile (formerly Atacama-1). This project showcases the feasibility and potential of similar storage systems in retrofitting retiring coal plants, offering a reliable source of renewable energy [2], [3]. In the context of the broader project "Decarbonization of the Energy Sector in Chile" implemented by the Ministry of Energy and Deutsche Gesellschaft für Internationale Zusammenarbeit (GIZ) GmbH, the publication [8] has been prepared, to explore a preliminary techno-economic analysis of retrofitting a coal plant in Chile (250 MWe net) with a CSP molten salt storage system, resistance heater and molten salt steam generator.

3 CASE ANALYSIS OF RETROFITTING AN EXISTING THERMAL PLANT, TEC NEGOTINO, WITH MOLTEN SALT STORAGE, RESULTS AND DISCUSSION

For the purpose of this conceptual analysis, it's important to highlight that the analysis in this section is based on the use of a typical daily profile. This approach was chosen to enhance our overall understanding, and to make it easier for us to compare different analysis variants, all within and under consistent conditions guided by techno-economic assumptions.

3.1 Technical Assumptions

The study utilizes Fig. 4 as the example configuration used in the techno-economic analysis for the possibility of retrofitting TEC Negotino, a 210 MWe (net) heavy-oil plant. Fig. 4 showcases the integration of an electrical salt heater, thermal capacity storage and a molten salt steam generator in the retrofitting process for TEC Negotino. A crucial step in the retrofitting involved replacing the heavy oil-fired boiler with an efficient molten salt steam generator, utilizing discharge heat from the molten tank storage to power the turbine generator.

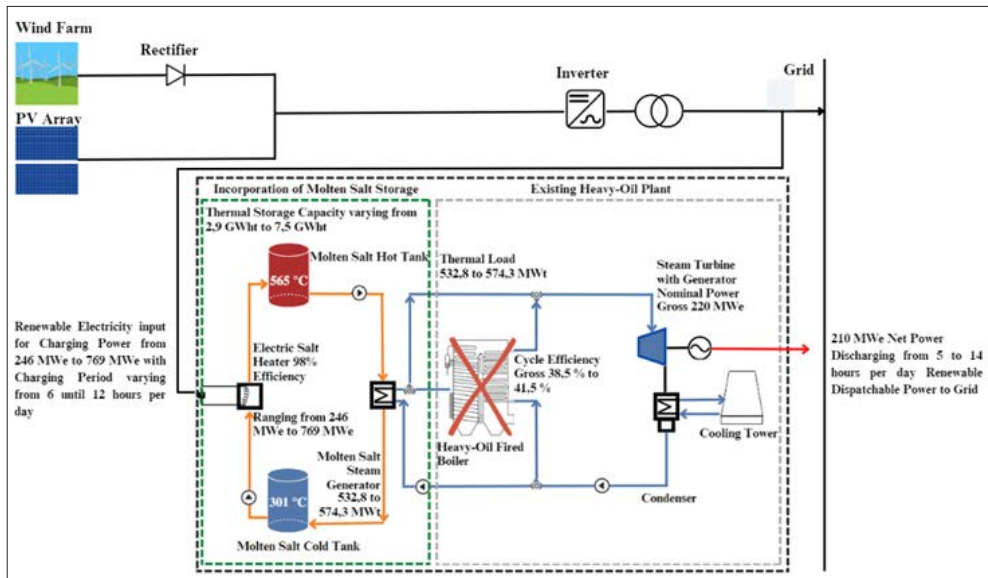


Figure 4: Incorporation of an MSTES system with thermal capacity varying from 2,9 GWht to 7,5 GWht to an existing heavy-oil plant of the 210 MWe class (net) in TEC Negotino – example configuration used in the techno-economic analysis

For the example configuration in Fig.4, the following component efficiencies were considered:

- Electric salt heater with an efficiency of 98%.
- Thermal energy storage tank with an efficiency of 99%.
- Molten salt steam generator with an efficiency of 99,5%.

Regarding the Rankine cycle gross efficiency for all analysis variants (Table 1), they were varied as follows:

- For variants V1-V3, the gross cycle efficiency was 38,5%.
- For variants V4-V7, the corresponding gross cycle efficiencies were 39%, 40%, 41% and 41,5%.

The capacity of the molten salt steam generator is always at full load for the specified discharge hours:

- For variants V1-V3 – constant capacity of approximately 574,3 MWt.
- For variants V4-V7 - capacities of approximately 566,9 MWt, 552,8 MWt, 539,3 MWt and 532,8 MWt, respectively.

Table 1 provides a summary of the sensitivity variants. In the next step, we analysed the sensitivity of annual energy yield, load factor, total investment cost and levelized cost of discharge electricity with varying the discharge duration, thermal storage capacity and charging duration.

Table 1: Sensitivity variants of discharging duration (full load hours), thermal storage capacity, charging duration and capacity of electric salt heaters

Sensitivity variant	Unit	V1	V2	V3	V4	V5	V6	V7
Discharging duration	[hours]	5	5	5	9	11	12	14
Thermal storage capacity	[GWht]	2,9	2,9	2,9	5,2	6,1	6,5	7,5
Charging duration	[hours]	6	8	12	10	11	11	10
Charging electric salt heater capacity	[MWe]	493,283	369,962	246,642	525,916	569,742	606,3774	768,808

At first, the discharging duration was varied, maintaining a constant 5 full load hours for the initial three variants (V1-V3), and extending to 9, 11, 12 and 14 full load hours for variants V4-V7. The corresponding thermal storage capacity ranged constant, with 2900,5 MWht for variants V1-V3; to 5153,98, 6141,8, 6536,75 and 7534,32 MWht for variants V4-V7, resulting in a plant load factor spanning from 20,8% for a 5-hour discharging duration to 37,5%, 45,8%, 50%, and 58,3% for 9, 11, 12 and 14-hour discharging durations, respectively. The plant load factor was determined using the following equation:

$$\text{Plant load factor} = \frac{\text{Average load}}{\text{Maximum demand}} \times 100 \text{ [\%]} \quad (3.1.1)$$

where, for daily calculations,

$$\text{Average load} = \frac{\text{Energy generated per day}}{24} \text{ [MW]} \quad (3.1.2)$$

and maximum demand was a maximum load of 210 MW.

Second, the charging duration, was directly proportional to both the installed capacity of the electric salt heaters and the thermal storage capacity. The charging duration was varied with 6, 8, 12 charging hours for the first three variants V1-V3 varying the corresponding electric salt heater capacity with 493,283, 369,962 and 246,642 MWe. The variants V4-V7 were varied with 10, 11, 11 and 10 charging hours, varying the corresponding electric salt heater capacity from 525,916, 569,742, 606,3774 and 768,808 MWe. The equation representing the conversion of charging electric salt heater power capacity [MWe] to nominal thermal power [MWt] considering the efficiency of the electric salt heater $\eta_{\text{el.salthheater}} = 98\%$ was as follows:

$$\text{Nominal thermal power} = \text{Charging electric salt heater capacity} \times \eta_{\text{el.salthheater}} \text{ [MWt]} \quad (3.1.3)$$

After determining the nominal thermal power, the thermal storage capacity was calculated by multiplying the nominal thermal power by the charge duration t_{charge} [hours], expressed as:

$$\text{Thermal storage capacity} = \text{Nominal thermal power} \times t_{\text{charge}} \text{ [GWht]} \quad (3.1.4)$$

Furthermore, the results encompassed the annual charging and discharging net electricity amounts, alongside the corresponding annual roundtrip charging/discharging efficiencies, which are represented visually in Fig. 5.

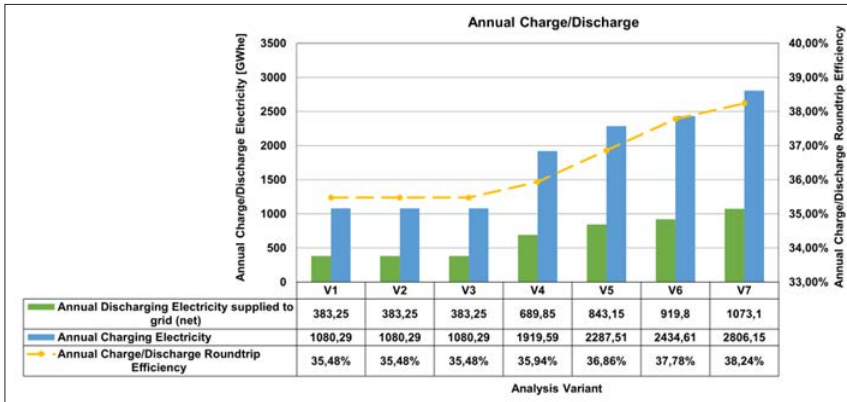


Figure 5: Chart representation of annual charging/discharging electricity and annual roundtrip charging/discharging efficiency for the analysis variants

The annual charging and discharging net electricity are determined based on typical daily profiles for the considered variants, utilizing the following equations:

$$\text{Annual discharge net electricity} = \text{Net power} \times \text{Discharge duration} \times 365 \text{ days [GWh]} \quad (3.1.5)$$

$$\text{Annual charge electricity} = \text{Charging electric salt heater capacity} \times \text{Charge duration} \times 365 \text{ days [GWh]} \quad (3.1.6)$$

The roundtrip efficiency ($\eta_{\text{roundtrip}}$) can be calculated using the provided equations for annual discharge net electricity and annual charge electricity. It is calculated as the ratio of the net electricity discharged to the grid over the year to the total electricity for charging the electric salt heater over the year:

$$\eta_{\text{roundtrip}} = \frac{\text{Annual discharge net electricity}}{\text{Annual charge electricity}} \times 100 [\%] \quad (3.1.7)$$

Notably, from Fig. 5, our observations highlighted variants V6 and V7 as the most favorable, achieving the best annual round-trip charging/discharging efficiencies at around 38%.

3.2 Assumptions in Investment Costs (CapEx) and Operation Costs (OpEx)

In this research, specific economic parameters, including investment and operational costs, were sourced from [8]. The key financing and cost parameters are presented in Table 2 and Table 3 for retrofitting molten salt storage in the existing heavy-oil plant TEC Negotino. In the context of this conceptual analysis, we assumed that the existing grid connection requires no modifications. Furthermore, the power plant in focus operates exclusively on non-fossil fuel, eliminating the need for specified fuel costs in our analysis. Moreover, we have set a constant charging rate from the grid at \$20 per megawatt-hour of electricity [MWh] for this analysis, regardless of its origin. In reality, such power is expected to originate primarily from a PV power plant. These assumptions are included in Table 2.

Table 2: Assumed specific investment cost for integrating molten salt storage for retrofitting an existing 210 MWe class heavy-oil plant

Specific investment cost	Unit	Value
Electric heater	[\$/kWe]	100
Storage system	[\$/kWht]	23
Solar salt	[\$/t]	Included in storage
HTF System		
Hot and cold salt pumps	[\$/kWt]	Included in storage
HTF piping system	[\$/kWt]	Included in storage
Heat tracing system	[\$/kWt]	Included in storage
Molten salt steam generator	[\$/kWt]	90
Power block including BOP (existing unit)	[\$/kWt]	0
Integration cost to existing Power Block	[\$/kWt]	10
Modification cost of grid connection	[\$/kWe]	0
Total surcharges (engineering, risk, management)	[%] of direct cost	30
Specific O&M cost		
O&M incl. insurance	[% of direct cost/y]	3
Fuel costs	[\$/MWh]	N/A
Electricity cost for charging	[\$/MWhe]	20

Fig. 6 shows the resulting total investment cost for seven different analysis variants (V1-V7).

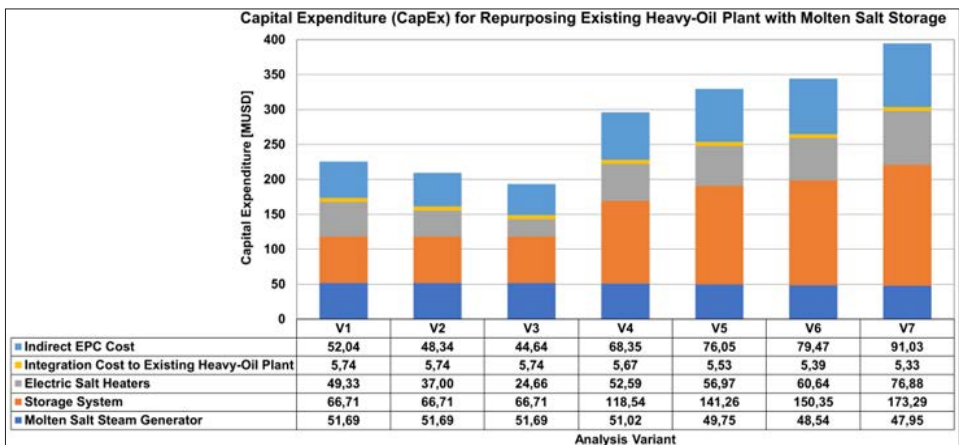


Figure 6: Chart representation of the estimated total investment cost (CapEx) for integrating a molten salt storage system (ERH+storage system+ molten salt generator) for retrofitting the existing heavy-oil plant TEC Negotino for the analysis variants (V1-V7)

In Fig. 6, for the analysis variant cases V1, V2 and V3, the constant capacity for the molten salt steam generator ($574,3 \times 10^3$ KWt) and storage system ($2900,5 \times 10^3$ KWht) (section 3.1) also represents a constant rounded investment cost of 51,69 and 66,71 million USD, correspondingly. The investment cost for the electric salt heater's capacity, varying with $493,283 \times 10^3$, $369,962 \times 10^3$, $246,642 \times 10^3$ KWe (Section 3.1), varied with values of 49,33, 37,00, 24,66 million USD respectively, rounded to two decimal places (also shown in Fig.6).

For the analysis variant cases V4, V5, V6 and V7, the investment cost for the molten salt steam generators capacity varied (Fig.6), with the values of 51,02, 49,75, 48,54 and 47,95 million USD, respectively. These values correspond to the molten salt steam generator's capacity of $566,9 \times 10^3$, $552,8 \times 10^3$, $539,3 \times 10^3$ and $532,8 \times 10^3$ KWt (section 3.1). The investment cost for the molten salt storage system in these analysis variant cases (Fig.6) also varied, with values of 118,54, 141,26, 150,35 and 173,29 million USD, respectively. These values correspond to the thermal storage capacity (in full load storage duration; section 3.1) with $5153,98 \times 10^3$, $6141,8 \times 10^3$, $6536,75 \times 10^3$, and $7534,32 \times 10^3$ KWht. In line with the varying storage capacity and charging duration (10 hour charging duration for V4 and V7; 11 hour charging duration for V5 and V6), the electrical salt heater's capacity is $525,916 \times 10^3$ KWe for V4, $569,742 \times 10^3$ KWe for V5, $606,3774 \times 10^3$ KWe for V6 and $768,808 \times 10^3$ KWe for V7 (section 3.1). These values of the electric salt heater's capacity for analysis variant cases V4, V5, V6 and V7 corresponded with the investment cost of 52,59, 56,97, 60,64 and 76,88 million USD respectively (as shown in Fig.6). The investment costs for individual components are rounded to two decimal places.

The integration cost to the existing heavy-oil plant and indirect EPC cost (30% of the direct cost) were considered for each analysis variant case. The resulting rounded total investment cost was the sum of the individual rounded investment analysis variants costs. The resulting rounded total investment cost (CapEx) for analysis variant cases (V1 to V7), shown in Fig.6, are as follows: 225,51, 209,48, 193,44, 296,17, 329,56, 344,39 and 394,48 million USD, respectively.

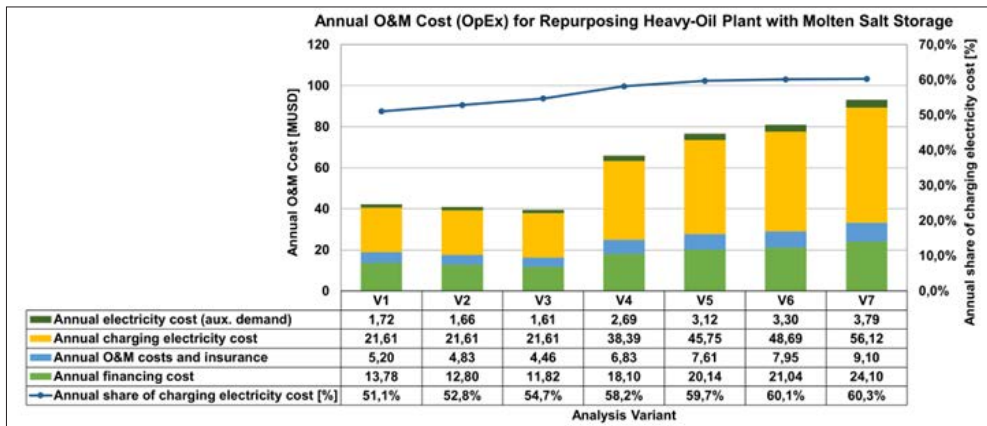


Figure 7: Chart representation of the estimated annual operation cost (OpEx) for integrating the molten salt storage system (ERH+storage system+ molten salt generator) for retrofitting the existing heavy-oil plant TEC Negotino for the analysis variants (V1-V7)

In the calculation of the annual operational cost shown in Fig. 7, the analysis relied on the following preliminary simplified assumptions:

1. A fixed cost of \$20 per megawatt-hour (\$/MWh) for charging electricity (Table 2), which may see a potential reduction in the future, especially when considering dedicated large-scale PV systems for storage charging. Presented in Fig. 7, the annual charging electricity cost varies from a constant value of 21,61 million USD for the first three analysis variants cases (V1 to V3) to 38,39, 45,75, 48,69 and 56,12 million USD for analysis variants cases (V4 to V7).
2. The annual O&M cost, including insurance, were estimated at 3% per annum of the corresponding CapEx. It is crucial to validate this estimate against actual O&M service offers. The annual O&M costs, including insurance, varied, with values of 5,20, 4,83, 4,46, 6,83, 7,61, 7,95 and 9,10 million USD for the analysis variants cases (V1 to V7), as shown in the chart representation in Fig.7.
3. The financing cost was determined through a simplified levelized cost of electricity (LCOE) analysis, assuming complete (100%) financing over a 35-year debt period with a constant real discount rate of 5%. The values presented in Table 3 need to be validated against real project finance offers. From there, the annuity of 6,11% in Table 3 was determined, using the following equation:

$$\text{Annuity} = i \times 1 + i n 1 + i n - 1 \times 100 \quad [\%] \quad (3.2.1)$$

Where,

i: periodic discount rate;

n: year debt period. The annual financing cost varied, with values of 13,78, 12,80, 11,82, 18,10, 20,14, 21,04 and 24,10 million USD for the analysis variants cases (V1 to V7), as shown in Fig. 7.

4. The auxiliary power consumption, determined at 4.05% of gross electricity production for our analysis, was used to estimate the cost of auxiliary power by consumption percentage and cost of discharging electricity. Values for the annual electricity cost, presented in Fig. 7, for auxiliary demand, varied with approximately 1,72, 1,66, 1,61, 2,69, 3,12, 3,30 and 3,79 million USD for the analysis variants cases (V1 to V7) .

In Fig. 7, we also observe a significant trend in the share of charging electricity cost in the total annual O&M cost across all seven analysis variants cases (V1 to V7). For the first three analysis variants cases (V1 to V3), with a 5 hour full load discharge duration, the respective share of charging electricity cost was 51,1%, 52,8%, and 54,7%. For the remaining four analysis variants cases (V4 to V7) with 9, 11, 12, and 14 full load discharge durations, the respective share of charging electricity cost was 58,2%, 59,7%, 60,1%, and 60,3%.

3.3 Levelized Cost of Discharge Electricity

Using the results of the energy yield and the annual cost of the power plant, the levelized cost of electricity could be calculated using the defined economic model in Fig. 8. This allows ranking of the various analysis variants cases. Some other economic parameters, such as taxes, project financing concepts, etc. have not been taken into account for this ranking. In our ranking analysis, we've gathered and outlined the financial assumptions in Table 3.

Table 3: Assumed financing data for calculating the levelized cost of discharge electricity

Financing data for LCOE	Unit	Value
Debt period	years	35
Discount rate	%	5,0
Annuity	%	6,11

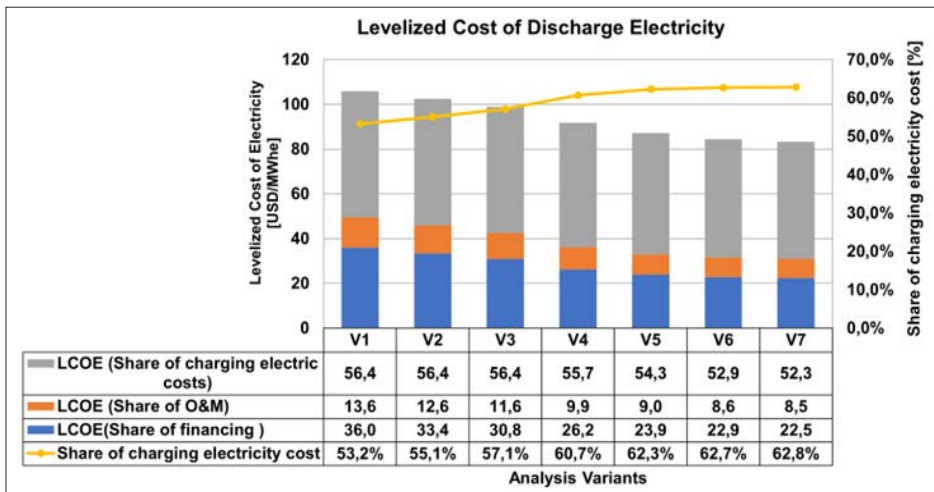


Figure 8: Chart representation of the levelized cost of discharge electricity for integrating a molten salt storage system (ERH+storage system+ molten salt generator) for retrofitting the existing heavy-oil plant TEC Negotino for the analysis variants (V1-V7)

In the analysis of levelized cost of discharge electricity (LCOE) for various analysis variants cases (V1 to V7) considering the potential conversion of the heavy-oil plant TEC Negotino into an MSTES plant, the results depicted in Fig. 8 reveal a distinctive ranking. The LCOE for a 5-hour full load discharge duration falls within the range of approximately 99 to 106 USD/MWhe. However, for longer discharge duration, the LCOE exhibited a decline, reaching approximately 92 USD/MWhe for a 9-hour full load discharge duration (V4), 87 USD/MWhe for an 11-hour full load discharge duration (V5), 84 USD/MWhe for a 12-hour full load discharge duration (V6) and 83 USD/MWhe for a 14-hour full load discharge duration. Additionally, the percentual shares of charging electricity to the overall LCOE is shown in Fig. 8, are 53,2%, 55,1%, 57,1%, 60,7%, 62,3%, 62,7% and 62,8% for the analysis variants cases (V1 to V7).

4 CONCLUSION

In conclusion, it is crucial to emphasize that this study represents a conceptual analysis conducted under consistent conditions, utilizing a typical daily profile for enhanced comparability. The chosen approach provided valuable insights into the techno-economic aspects of the possibility of retrofitting the 210 MW thermal heavy-oil power plant, TEC Negotino, with a molten salt thermal energy storage system (a Carnot battery). The study explores the sensitivity of various parameters, based on the techno-economic assumptions, to estimate the possibility of integrating the proposed system. The results indicate that longer discharging durations, specifically for analysis variants V6 and V7 with 12 and 14 full load hours, resulted in the most favorable annual roundtrip efficiencies and lower levelized cost of discharging electricity. Analysis variants V6 and V7 emerged as particularly promising, achieving around 38% annual roundtrip charging/discharging efficiency and levelized cost of discharging electricity below 90 USD/MWhe, approximately 84 USD/MWhe for a 12-hour full load discharge duration (V6) and 83 USD/MWhe for a 14-hour full load discharge duration (V7). This possibility not only emphasizes the potential for the thorough decarbonization of TEC Negotino, but also focuses on conserving the majority of power plant jobs.

As next steps, it is recommended to conduct a detailed engineering study with a dynamic profile on the proposed retrofitting of a molten salt storage facility with electric salt heaters and molten salt steam generators in the existing heavy-oil plant TEC Negotino, in order to obtain commercial offers and investigate the financing possibilities for such a measure.

References

- [1] **A. Vecchi, K. Knobloch, T. Liang, ..., Y. Ding:** *Carnot Battery development: A review on system performance, applications and commercial state-of-the-art*, Journal of Energy Storage, Vol. 55, Part D, 2022
- [2] **M. Geyer:** *CSP and Thermal Energy Storage*, Seminario "Concentración Solar de Potencia, una Opción Clave para la Transición Energética" Santiago de Chile, April 25, 2019
- [3] **World Bank:** *Concentrating Solar Power: Clean Power on Demand 24/7*, Washington, DC, 2021
- [4] Koalitionsvertrag zwischen CDU, CSU und SPD, 2018
- [5] **M. Geyer, C. Prieto:** *20 - Storing energy using molten salts*, Storing Energy (Second Edition), p.p. 445-486, 2022
- [6] **W. Arnold, S. Giuliano, T. Bauer, M. Geyer, DLR, RWE, ..., S. Zunft:** *StoreToPower: Stromspeicherung in Hochtemperatur-Wärmespeicherkraftwerken*, öffentlicher Abschlussbericht, p.p. 1-161, 2022
- [7] **M. Geyer, S. Giuliano:** *Conversion of Existing Coal Plants Into Thermal Storage Plants*, Applied Sciences, In: Luisa F. Cabeza (eds.), Encyclopedia of Energy Storage, Vol. 2, p.p. 122-132, 2022

- [8] **M. Geyer, F. Trieb, S. Giuliano:** *Reconversión de centrales a carbón en plantas de almacenamiento térmico con energía renovable en Chile*, Executive Summary, p.p. 1-27, 2020
- [9] **J. Li, W. Qi, J. Yang, Y. He, J. Luo, S. Guo:** *The Capacity Optimization of Wind-Photovoltaic-Thermal Energy Storage Hybrid Power System*, ICAEER, E3S Web of Conferences 118, 02054, 2019
- [10] **T. Bauer, C. Odenthal, A. Bonk:** *Molten Salt Storage for Power Generation*, Chemie Ingenieur Technik, Vol.93 (4), p.p. 534-546, 2021
- [11] **Gibb et al. from the German Aerospace Center (DLR):** *Applications of Thermal Energy Storage in the Energy Transition – Benchmarks and Developments*, , IEA Technology Collaboration Programme on Energy Conservation through Energy Storage (IEA-ECES), 2018

METHODS FOR RECYCLING PHOTOVOLTAIC MODULES AND ELEMENT RECOVERY PROJECTIONS IN SLOVENIA

METODE RECIKLIRANJA FOTOVOLTAIČNIH MODULOV IN PROJEKCIJE ZA PRIDOBIVANJE ELEMENTOV V SLOVENIJI

Manja Obreza ^{1✉}, Nejc Friškovec ¹, Klemen Sredenšek ¹, Sebastijan Seme ^{1,2}

Keywords: photovoltaic modules, photovoltaic modules` recycling, waste management, end-of-life cycle

Abstract

This paper aims to present different methods of recycling photovoltaic modules, which were researched by different institutes. Significant importance has been attributed to photovoltaic modules in the Renewable Energy sector, thereby contributing to the global transition towards sustainable energy sources. However, as the lifespan of these modules comes to an end, effective recycling methods will become crucial to minimize the environmental impact and resource depletion. This paper highlights recent advancements in photovoltaic module recycling technologies, focusing on predicting the potential mass of a specific element that could be recovered through recycling in Slovenia, considering the installed capacity of solar power plants, which is approximately 1105 MW. A projection of materials that can be obtained through the recycling process of photovoltaic modules was conducted based on current installed capacity, and it was discovered that up to 2150 tons of silicon and 1025 tons of copper could be obtained by the recycling process. The acquisition of various materials would have a significant role in the production of new photovoltaic modules, thereby enabling sustainable manufacturing and contributing substantially to the circular economy.

✉ Corresponding author: Manja Obreza, E-mail address: manja.obreza@student.um.si

¹ University of Maribor, Faculty of Energy Technology, Krško, Slovenia

² University of Maribor, Faculty of Electrical Engineering and Computer Science, Maribor, Slovenia

Povzetek

V članku so predstavljene različne metode reciklaže fotovoltaičnih modulov. Fotovoltaični moduli so v sektorju obnovljive energije izjemno pomembni, saj prispevajo h globalnemu prehodu k trajnostnim energetskim virom. Čeprav imajo relativno dolgo življenjsko dobo, se tudi ta s časom izteče, zato je vse bolj nujno odkriti učinkovite metode recikliranja, saj so ključne za zmanjšanje okolijskih vplivov in izčrpanja virov. V tem članku so poudarjeni nedavni napredki v tehnologiji reciklaže fotovoltaičnih modulov, pri čemer je pomembna projekcija potencialne mase določenih materialov, ki jih je možno pridobiti v procesu reciklaže ob upoštevanju inštalirane moči fotovoltaičnih elektrarn, ki trenutno znaša okoli 1105 MW. Iz rezultatov projekcije materialov je bilo ugotovljeno, da bi lahko s postopkom pridobili do 2150 ton silicija in 1025 ton bakra. Pridobitev različnih materialov bi imela pomembno vlogo pri proizvodnji novih fotovoltaičnih modulov, saj bi omogočila trajnostno proizvodnjo in bistveno prispevala h krožnemu gospodarstvu.

1 INTRODUCTION

Photovoltaic (PV) technology stands out as a highly promising solution for bolstering energy security and combating climate change. Its market is experiencing swift growth, with projections indicating continued expansion globally. The anticipated global photovoltaic installed capacity is set to reach approximately 4500 GW by 2025 [1]. Beyond its evident benefits for energy security and climate resilience, PV technology distinguishes itself as one of the eco-friendliest options among all the energy and electricity generation methods. This is particularly evident when considering its entire life cycle, including end-of-life (EOL) handling. Therefore, ensuring proper management at end of its lifespan becomes imperative for maintaining the integrity of “clean” energy technologies [2].

One of the primary challenges in recycling PV modules is the lack of standardized recycling procedures, which underscores the importance of implementing appropriate regulatory and technological approaches tailored to the conditions of each country. The European Union (EU) is one of the associations that has already adopted specific Directives in this area, whereas, in other parts of the world, legislation is not defined or even developed adequately. The Waste from Electrical and Electronic Equipment (WEEE) Directive introduces laws pertaining to the recycling of electrical and electronic equipment aimed at enhancing sustainable production and resource efficiency to contribute to the circular economy. The Directive mandates that all WEEE, including PV modules, must be recycled and processed in accordance with specific Standards. Furthermore, it stipulates that manufacturers and importers of equipment are legally responsible for their recycling, and ensuring that their disposal aligns with the Environmental Standards. The first Directive that acknowledged detailed provisions for the EOL management of PV modules was 2012/19/EU. The law also stipulated that all European member states are required to establish systems for the collection and treatment of PV modules in compliance with this Directive. Manufacturers are also obligated to report monthly or annually on the number of PV modules sold. Within these reports, the result of waste management activities must also be presented, encompassing the mass of materials processed, recycled, or disposed of, such as glass, mixed plastic waste, metals, etc. Furthermore, accountability for informing customers about the management of PV modules at the EOL is also assigned to them [3].

Silicon (Si), as a semiconductor, is utilized most crucially in the production of PV modules, which are key for the generation of electricity. In general, three types of PV cells are distinguished:

monocrystalline, polycrystalline and amorphous solar cells.

Monocrystalline PV cells are made from a single crystal of high-purity silicon obtained from a cylindrical ingot. The ingot is sliced into wafers, each exhibiting a diamond-like crystal structure. Silicon extraction from silica sand begins in arc furnaces, and undergoes purification steps to remove impurities, resulting in polysilicon. The final production of monocrystalline silicon involves the costly Czochralski process, yielding an ingot. These ingots are cut into wafers used for solar cell production, known for their high efficiency ranging from 17% to 22% compared to other PV modules.

Polycrystalline PV cells are manufactured similarly to monocrystalline PV cells, but with a notable difference. Instead of bonding multiple grains of monocrystalline silicon together to form wafers, multiple grains of monocrystalline silicon are bonded together in polycrystalline cells. This variation earns them the designation of multi-crystalline PV cells. However, this configuration restricts the flow of electrons, resulting in lower efficiency compared to monocrystalline modules. Efficiency ranges typically from 15% to 17% in polycrystalline modules, although advancements in technology are narrowing the gap with monocrystalline PV modules.

Amorphous PV cells are manufactured similarly to integrated circuits, with thin semiconductor layers deposited on glass, plastic, or metal substrates. Various materials are used, including amorphous silicon, cadmium telluride, gallium arsenide, and copper indium gallium selenide. Despite varying efficiencies, ranging typically from 10% to 20%, they offer flexibility and reduced weight. Broad light spectra are absorbed effectively by amorphous silicon. Minimal risks are posed by cadmium telluride, despite its toxicity. Efficiency under temperature fluctuations is maintained by gallium arsenide, making it suitable for concentrator PV systems. Copper indium gallium selenide boasts the highest efficiency among thin-film materials, requiring thinner films due to its high absorption coefficient [4-8].

PV modules can be made from various materials; however, most of the market is based on monocrystalline silicon cell technology, which, typically, has a thickness between 150 and 180 μm . A monocrystalline PV module is composed of silicon cells, an antireflective layer of silicon nitride (SiN_x), with the front electrode made of silver and the back electrode made of aluminum [9].

Monocrystalline PV modules consist of the following mass fractions of materials, as presented in Table 1 [9].

Table 1: The mass friction of materials in PV modules [9]

Materials	Mass friction [%]
Glass	71,57
Polymer	12,68
Aluminum (Al)	10,30
Silicon (Si)	3,48
Copper (Cu)	1,77
Tin (Sn)	0,12
Lead (Pb)	0,07
Silver (Ag)	0,01

2 AN OVERVIEW OF METHODS FOR RECYCLING PV MODULES

Research and development in the technology focused on recycling monocrystalline silicon PV modules dates back to the 1990s, when the primary goal was to obtain Si cells without damaging them during the process. The recycling processes of PV modules are divided into thermal and chemical methods [10].

The thermal process, that has been known for several years, entails subjecting PV modules to heating in a furnace at elevated temperatures (between 500°C – 600°C) conducted in two phases. During the process, polymer materials undergo combustion or cracking, while Silicon cells, glass and metals are removed manually. All the obtained usable materials are subsequently processed through recycling, and can be employed in the manufacturing of new PV modules [11].

The chemical process involves the immersion of PV modules in solvents, after which the components are separated through various chemical reactions. The chemical process requires more time than the thermal process, but the percentage of undamaged silicon cells is higher. In the 1990s, BP Solar operated with nitric acid in the recycling process. After one day, ethylene-vinyl-acetate (EVA), a polymeric material that is used to protect PV cells, was dissolved, while the silicon cells and metals were separated and recovered. The silicon cells obtained can then be etched with sodium hydroxide, and reprocessed from silicon wafers into silicon cells. However, due to the formation of nitrogen oxide during the reaction, this recycling method was deemed not the most sustainable, and the disposal of waste acid posed another issue. The availability of organic solvents for separation was also explored as an alternative approach. It was found that many organic solvents could dissolve EVA, but, eventually, they were not suitable for thermal treatment [12, 13].

Recycling processes must meet current, as well as anticipated, future requirements. They must adhere to Regulations for higher levels of processing, and reduce the environmental impact caused by waste PV modules and their processing methods. The current technological development focuses primarily on removing the EVA encapsulant from the laminated structure, separating the glass and other materials, and extracting metals from the Si cells and electrodes. In some cases, efficient removal of the aluminum (Al) frame and junction box is also included in the process before removing the encapsulant itself. Nevertheless, the extraction of the encapsulant remains the most formidable aspect of the PV module recycling procedure. Recent technological advancements in recycling procedures are categorized into thermal, chemical, and mechanical processes [2]. Figure 1 illustrates the scheme of currently researched recycling processes for monocrystalline silicon (Si) PV modules.



Figure 1: Diagram of current advancements in processes for recycling monocrystalline silicon PV modules

The technical potential of the thermal process has been confirmed through research in its preliminary stages. For example, the FAIS (Kitakyushu Foundation for the Advancement of Industry, Science, and Technology, Japan [14]) has developed PV module recycling technology which includes a process for removing the aluminum frames, back layers, and thermal degradation of EVA encapsulation. To manage PV modules, they employed a system controller that coordinated loading and unloading for PV modules, enabling automatic processing, from loading all the way to the recovery of valuable materials. The first step involves removing the Al-frame using an air actuator. The milling machine removes the back layer to prevent glass cracks in further cracks, and is disposed of as industrial waste. The PV modules, without the Al-frame and back layer, are heated, and the EVA encapsulation is degraded thermally in an oven, with the gas generated during the process being suctioned and incinerated. The oven is preheated to 350 °C, then heated to 500 °C, and, finally, cooled down to 250°C. The heat generated during the combustion of the EVA layer is utilized in the oven heating process. All components, including glass, silicon cells, and electrodes, are recovered after the three main steps. The technology is suitable for processing commercial modules on the market, with a processing rate of approximately 12 MW/year, depending on the module size. The recycling efficiency is nearly 95 %. The obtained glass can be processed into float glass without excessive fragmentation. The process of extracting metals from silicon cells and electrodes is not included in this type of technology. In addition, the technology developed by Chonnam National University [15] involves a thermal process for separating the laminated structure and a chemical process for metal recovery. Nitric acid and sodium hydroxide are used in the chemical process of ultrasonic treatment. After the process, the silicon is purified to 99.998 % purity using the CaO-CaF-SiO₂ compound at 1520 °C.

Currently, a mechanical process is employed in Europe for extracting glass from waste PV modules. The process involves crushing the glass, scraping off layers and cutting the encapsulating layer. Additionally, the procedures encompass the removal of the laminated structure, followed by steps to separate the glass and polymers. For instance, the Sapienza University of Rome [16] has developed an automatic crushing process, which involves manual removal of aluminum frames, automatic crushing of laminated structures and separation of glass for metal processing. Two different crushing methods were evaluated, the first involving crushing with a dual-rotor system, while the second method combined dual-rotor crushing with hammer milling, which appeared more suitable based on the analysis of the distribution of crushed module structures. Crushed particles can be processed in three ways, depending on the diameter (d), presented in Table 2.

Table 2: Processing of crushed particles [16]

Diameter of particle	Process
$d > 1 \text{ mm}$	Incineration process at 650 °C to separate polymers.
$1 \text{ mm} > d > 0.08 \text{ mm}$	Direct glass recovery.
$d < 0.08 \text{ mm}$	Processing with a hydro-metallurgical method for metal recovery.

Chemical processes were already being utilized in the preliminary stages of research of procedures for recycling PV modules. However, it was found that many of them needed refinement, as they were found to impose significant environmental burdens with gas and liquid emissions, leading to the development of numerous new technologies. Chemical processes typically require prolonged treatment, which makes them unsuitable for mass processing.

The Yokohama Oils & Fats industry [17] has developed solvents and processes for removing the casing from laminated structures. Initially, aluminum frames and connection boxes are removed manually, while the casing is stripped away mechanically. The remaining laminated structure is then immersed in a neutral solvent, to separate the glass, EVA layer, silicon cells, and electrodes. If the separated glass is undamaged, it can be reused; however, if it is damaged, it undergoes the recycling process. The next layer is crushed and immersed in an alkaline solvent, from which the EVA layer, silicon, and electrodes are obtained after immersion. An additional process is required to obtain silver. The expected processing time is one day, due to the soaking process in solvents, which is the main drawback of this method. The main advantage is that the developed solvents are environmentally friendly, and the process could be made even more efficient by combining it with a mechanical process.

The Korean Research Institute of Chemical Technology (KRICT) and Kangwon National University [18] have developed a process for dissolving EVA by immersing modules in an organic solvent and subjecting them to additional ultrasonic (UV) irradiation. The aim of UV irradiation is to shorten the time of chemical separation. EVA plastic dissolves at 70°C and at an irradiation power of 900 W, while silicon cells are obtained without damage. In both technologies, after removing the casing from the laminated structure, an additional process is required to extract the metals from the silicon cells.

3 RESULTS

A review of the installed capacity of photovoltaic systems has been conducted, examining the main reasons for the growth or decline in installation. As will be evident later in the paper, photovoltaic power plants were initially installed with declarations, with self-sufficient installations only becoming active from 2015 onwards. Figure 2 presents the annual installed capacity and the total installed capacity of PV systems.

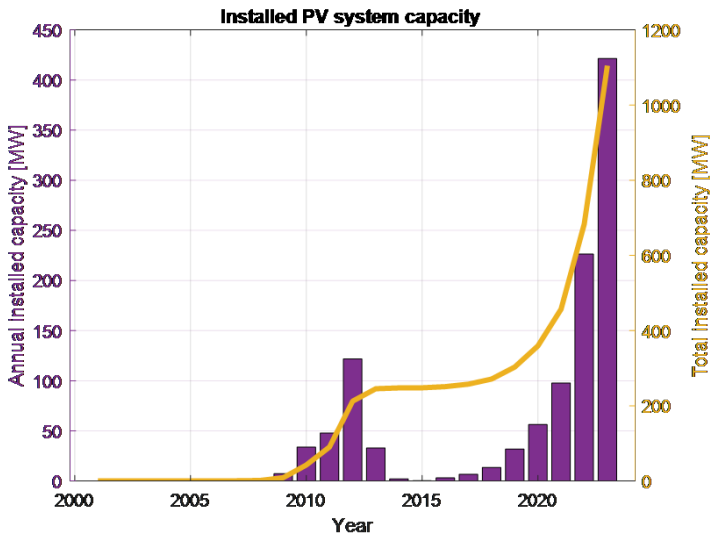


Figure 2: Installed capacity of PV systems by individual years in Slovenia

It can be observed that there has been an exponential increase in the installed capacity of PV systems. This growth is also driven by Slovenia's set target for the share of renewable energy sources in gross final energy consumption, with a goal of achieving 35 % renewable energy by 2030.

Figure 3 shows the installed capacity of PV systems with certification by individual years in Slovenia.

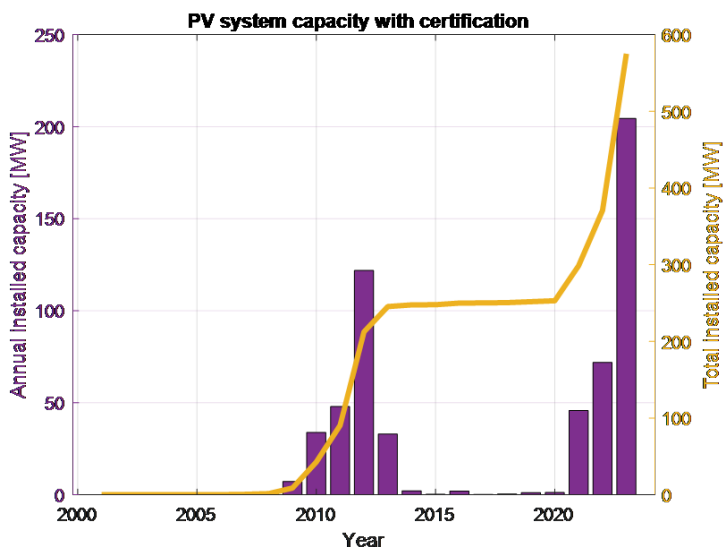


Figure 3: Installed capacity of PV systems with certification by individual years in Slovenia

In 2009, the government approved the installation of PV systems with certification (Figure 3), as the investment for installation was low, and the payout per kWh was favorable. The installed solar power plants were categorized based on capacity into:

- Micro power plants (up to 50 kW) – with an electricity purchase price of 0.41546 €/kWh;
- Small power plants (up to 1 MW) – with an electricity purchase price of 0.38002 €/kWh;
- Medium power plants (up to 5 MW) – with an electricity purchase price of 0.31536 €/kWh.

The state boosted interest in PV systems` construction significantly by offering investors higher purchase prices and extending the guaranteed purchase period. Regulations in 2011 proposed a reduction in production facility costs, affecting fixed and variable reference costs. Subsequently, in 2012, support for PV production facilities connected to the grid was reduced drastically, leading to a notable decline in solar power plant installations in 2013. The introduction of a tender system for promoting renewable energy sources through the 2014 Energy Act aimed to address this issue, alongside emerging initiatives for net metering to facilitate small private investments in PV systems, particularly concerning retirees facing pension repayment demands during operation [20 – 24].

At the end of 2015, the government adopted a new Regulation on self-sufficiency of PV systems (UL RS, No. 97/2015). This Regulation outlines the conditions for self-sufficiency with electricity generated from RES, the method of calculation, annual power limits for self-sufficiency devices, reporting requirements for the implementation of the measure, and the method of calculating the electricity produced by self-sufficiency devices. The Regulation defined the maximum rated power of a self-sufficiency device at 11 kVA, which could not exceed the connection power specified in the connection consent. Furthermore, the calculation method was established, whereby the amount of electricity credited to the owner of the self-sufficiency device corresponds to the difference between the consumed and delivered working electricity, as measured at the same metering point at the end of the billing period. Surpluses of produced electricity will not incur charges. If, at the end of the billing period, the amount of electricity delivered to the grid through the metering point exceeds the amount of consumed working electricity, the excess amount of working electricity is transferred to the supplier's account without charge. The Regulation came into effect on January 15, 2016 [20, 21, 22, 25].

In 2016, slightly over 3 MW of new PV systems were installed, with one-third of these systems being installed for self-sufficiency purposes. The government of the Republic of Slovenia issued the Regulation on Energy Infrastructure (UL RS, No. 22/2016), which eliminated the requirement for government approval for registration and deletion in the Infrastructure Registry. The most significant change introduced by this Regulation was for investors planning to install electricity generation devices, who would have previously been required to submit Appendix 2 before connecting the device, a requirement that is no longer applicable [20, 21, 22, 26].

Figure 4 presents a very dynamic market for PV systems in 2017, with the majority of installations intended for self-sufficiency, following a few years of quiet in the solar power sector.

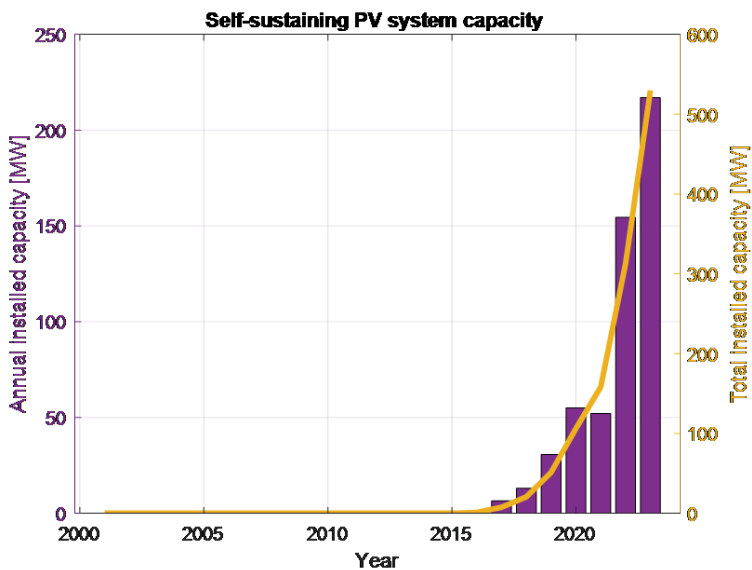


Figure 4: Installed capacity of self-sufficiency PV systems by individual years in Slovenia

In 2019, the rapid growth of self-sufficiency PV systems (Figure 4) continued under the self-sufficiency scheme, with an average and minimum offered price for electricity production from solar power plants at 75.71 €/MWh. The Regulation on self-sufficiency with electricity from renewable sources introduced the concept of "community self-sufficiency" for multi-apartment buildings and communities of renewable energy sources. In 2020, there was a further increase in small solar power plants for self-sufficiency, with almost 60% more installations than in 2019. The village of Luče in the Savinja Valley became Slovenia's first self-sufficient community, meeting its electricity needs fully from renewable energy. In 2021, approximately 56 MW of new solar power plants were installed, alongside a significant increase in electricity prices. In 2022, a total of 164 MW of solar power plants were installed, including the largest solar power plant to date, Prapretno, with an installed capacity of 3 MW. In March 2022, the Government of Slovenia issued a Regulation on self-supply with electricity from renewable energy sources, introducing new calculations for network charges, abolishing net metering for devices entering the self-supply system in 2024, simplifying procedures for devices up to 50 kW, and specifying that connections are considered approved if the distribution system operator does not issue decisions or rejections within one month. Self-supply consumers will be required to pay network charges for energy taken from the grid, but will not have to pay for energy fed into the grid [20-28].

Figure 5 shows the approximate number of PV modules in Slovenia, calculated based on the installed capacity of PV systems, and assuming that the average power of one module is 350 W.

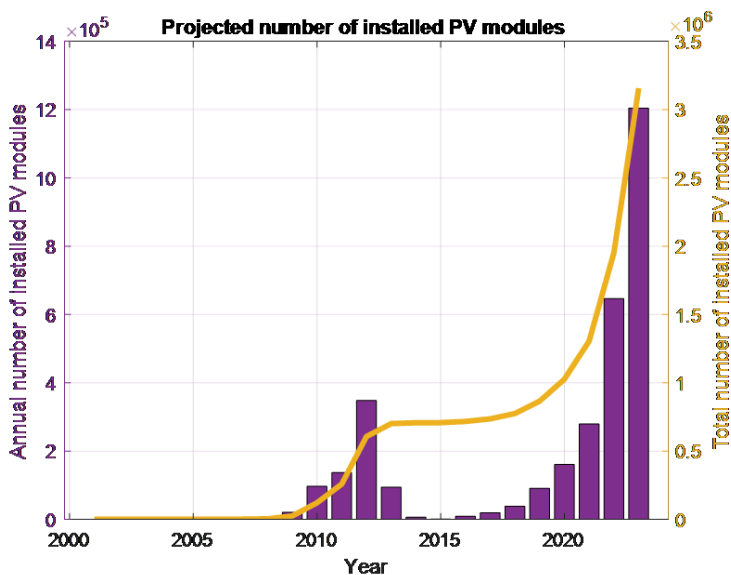


Figure 5: Projected number of installed PV modules

With the help of the projected number of modules (Figure 5) obtained by assuming that each PV module has an average power of 350 W, we aimed to illustrate the projected capacity of waste or recycled material in the future.

The authors in [9] cited the following average recycling factors for the materials shown in Table 3.

Table 3: Average recycling factors for materials in PV modules [9]

Material obtained through the recycling of PV modules	The factor of successfully recycled material
Glass	0,96
Aluminum (Al)	1
Silicon (Si)	0,91
Copper (Cu)	0,85
Silver (Ag)	0,95
Lead (Pb)	0,96
Tin (Sn)	0,32

With the proportions of materials in PV modules considered from Table 1, the predicted mass was calculated of elements or substances obtained after recycling. The data sheet in [29], where it is stated that a 300 W solar module weighs 18.5 kg, was used to introduce the mass equivalent, which is 61.6667 kg/kW. Using the mass equivalent, the predicted mass of obtained elements after the recycling process for each year was then calculated separately, based on the estimated number of PV modules.

Figure 6 presents element recovery projections in Slovenia.

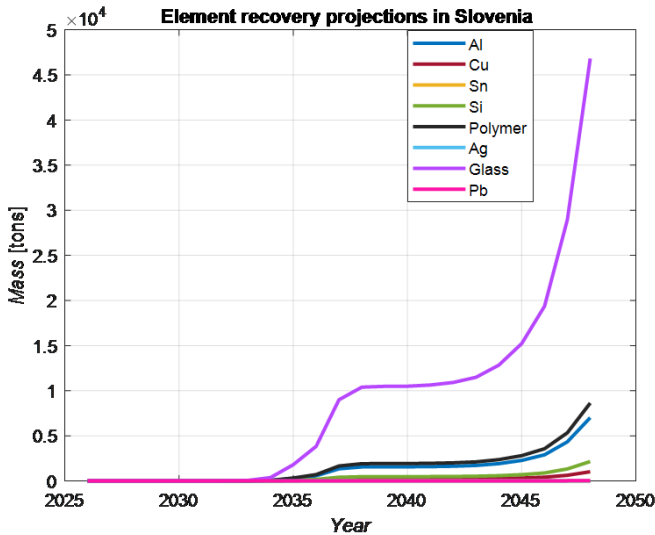


Figure 6: Element recovery projections in Slovenia

Figure 6 shows that the highest mass of glass, polymers, and aluminum can be yielded by the recycling process, as they constitute most of the PV module. With a 25-year lifespan assumed for PV modules and the first installations dating back to 2001, the initial modules eligible for recycling would be available in 2026. By 2048, approximately 46,818 tons of glass, 8,640 tons of polymers, and 7,018 tons of aluminum could be obtained, based on the current installed capacity

of 1105 MW. Elements such as silver, silicon, and copper will be crucial for the circular economy. According to our projection, based on the current installed capacity, 2,157 tons of silicon, 1,025 tons of copper, and approximately 6 tons of silver could be obtained for further use in production. However, significant optimization of the recycling processes is necessary, as the current purity of elements is not sufficiently high, and excessively aggressive chemicals are used in the process of obtaining silicon, copper, and silver.

4 DISCUSSION

This paper presented various methods of recycling PV modules. The main finding is the necessity for an effective recycling process, which includes mechanical, chemical, and thermal processes for optimal results. Currently, the most researched methods of recycling are those for monocrystalline PV modules, which are also the most widespread commercially. Despite the relatively recent emergence of recycling processes and associated legislation for PV modules, recycling technologies are already quite well-researched, but they will certainly be optimized further for improved efficiency, sustainability, and cost-effectiveness in the future. Additionally, the exponential growth of installed PV system capacity in Slovenia was described, along with the factors influencing it. A future decline in installed capacity is expected, due to economic factors. The acquisition of materials over 25 years was projected, based on data on the installed PV system capacity in Slovenia, factors of recycled materials, and known mass fractions of elements/materials in PV modules. The main finding was that significant quantities of useful materials could be obtained, such as silver, copper, and silicon. Additionally, a large amount of polymer, glass, and aluminum mass, which are the main constituent materials of PV modules, would be obtained as a result of recycling.

References

- [1] IRENA, IEA PVPS: *Renewable energy statistics 2023*, 2023
- [2] IRENA, IEA PVPS: *End-of-life-Management: Solar Photovoltaic Panels*, 2016
- [3] **Waste from Electrical and Electronic Equipment (WEEE)** Available: https://environment.ec.europa.eu/topics/waste-and-recycling/waste-electrical-and-electronic-equipment-weee_en (date of last access: 7. 3. 2024)
- [4] S. A. Kalogirou: *Photovoltaic Systems*, ScienceDirect, 2009
- [5] M. Prosenjak: *Investment analysis in photovoltaic system depending on different solar modules*, Diploma thesis, Univerza v Mariboru, Fakulteta za elektrotehniko, računalništvo in informatiko, 2014
- [6] M. Rizwan, W. S. Khan, S. Aleena: *Monocrystalline Silicon Solar Cells*, *Materials for Solar Cell Technologies I*, p.p. 148-175, 2021
- [7] S. Sharma, K. K. Jain, A. Sharma: *Solar Cells: In Research and Applications – A Review*, *Materials Sciences and Applications*, 6, p.p. 1145-1155, 2015. doi: 10.4236/msa.2015.612113

- [8] **A. Shah:** *Amorphous Silicon Solar Cells*, Solar Cells and Modules, p.p. 139-161, 2020. doi: 10.1007/978-3-030-46487-5_6
- [9] **A. Mulazzani, P. Eleftheriadis, S. Leva:** *Recycling c-Si PV Modules: A Review, a Proposed Energy Model and a Manufacturing Comparison*, Energies, 2022
- [10] **Bohland, J. R., et al.:** *Photovoltaics as Hazardous Materials: the Recycling*, 2nd WCPEC, 1998
- [11] **Frisson, L., et al.:** *Cost Effective Recycling of PV Modules and the Impact on Environment, Lifecycle*, Energy Payback Time, 2nd WCPEC, 1998
- [12] **Lee, J. -S.:** *Recovery Technology of Intact Wafer from End-of-life c-Si PV Module*, 26th PVSEC, 2016
- [13] **Doi, T., et al.:** *Experimental Study on PV Module Recycling with Organic Solvent Method*, 11th PVSEC, 1999
- [14] **M. Noda, K. Kushiya, H. Saito, K. Komoto, T. Matsumoto:** *Development of the PV recycling system for various kinds of PV modules*, 6th WCPEC, 2014
- [15] **Yi, Y. -K., et al.:** *Recovering Valuable Metals from Recycled Photovoltaic Modules*, J. of Air & Waste Management Association 64, p.p. 797-807, 2014
- [16] **Granata, G., et al.:** *Recycling of Photovoltaic Panels by Physical Operations*, Solar Energy Materials & Solar Cells 123, p.p. 239–248, 2014
- [17] **Yokohama Oils & Fats Industry:** *Development of an Advanced Recycling Treatment System for Photovoltaic Modules with Novel EVA Stripper*, Fiscal year 2011-2012 NEDO contract report, 2012
- [18] **Kang, S., et al.:** *Experimental investigations for recycling of silicon and glass from waste photovoltaic modules*, Renewable Energy 47, p.p. 152-159, 2012
- [19] **PVportal – slovenski portal za fotovoltaike.** Available: <http://pv.fe.uni-lj.si/sl/> (date of last access: 7. 3. 2024)
- [20] **Borzen.** Available: <https://www.borzen.si/sl/> (date of last access: 7. 03. 2024)
- [21] **Portal energetika – arhiv poročil.** Available: <https://www.energetika-portal.si/dokumenti/poslovna-porocila/porocilo-o-stanju-na-podrocju-energetike/> (date of last access: 7. 3. 2024)
- [22] **Javna agencija Republike Slovenije za energijo.** Available: <https://www.agen-rs.si/> (date of last access: 17. 02. 2024)
- [23] **he Constitution of the Republic of Slovenia.** The Official Gazette RS, No. 105/2011, 2011
- [24] **The Constitution of the Republic of Slovenia.** The Official Gazette RS, No. 17/2014, 2014
- [25] **The Constitution of the Republic of Slovenia.** The Official Gazette RS, No. 97/2015, 2015

- [26] **The Constitution of the Republic of Slovenia.** The Official Gazette RS, No. 22/2016, 2016
- [27] **The Constitution of the Republic of Slovenia.** The Official Gazette RS, No. 17/2019, 2019
- [28] **The Constitution of the Republic of Slovenia.** The Official Gazette RS, No. 43/2022, 2022
- [29] **ENF Solar – Solar Companies and Products, Mono 300 W.** Available: <https://www.ensolar.com/pv/panel-datasheet/crystalline/39841> (date of last access: 19 2. 2024)

Nomenclature

(Symbols)	(Symbol meaning)
<i>PV</i>	Photovoltaics
<i>EOL</i>	End-of-life
<i>EU</i>	European Union
<i>WEEE</i>	Waste from electrical and electronic equipment
<i>EVA</i>	Ethylene-vinyl-acetate



MAIN TITLE OF THE PAPER

SLOVENIAN TITLE

Author¹, Author², Corresponding author[✉]

Keywords: (Up to 10 keywords)

Abstract

Abstract should be up to 500 words long, with no pictures, photos, equations, tables, only text.

Povzetek

(Abstract in Slovenian language)

Submission of Manuscripts: All manuscripts must be submitted in English by e-mail to the editorial office at jet@um.si to ensure fast processing. Instructions for authors are also available online at <http://www.fe.um.si/en/jet/author-instructions.html>.

Preparation of manuscripts: Manuscripts must be typed in English in prescribed journal form (MS Word editor). A MS Word template is available at the Journal Home page.

A title page consists of the main title in the English and Slovenian language; the author(s) name(s) as well as the address, affiliation, E-mail address, telephone and fax numbers of author(s). Corresponding author must be indicated.

Main title: should be centred and written with capital letters (ARIAL bold 18 pt), in first paragraph in English language, in second paragraph in Slovenian language.

Key words: A list of 3 up to 6 key words is essential for indexing purposes. (CALIBRI 10pt)

[✉] Corresponding author: Title, Name and Surname, Organisation, Department, Address, Tel.: +XXX x xxx xxx, E-mail address: x.x@xxx.xx

¹ Organisation, Department, Address

² Organisation, Department, Address

Abstract: Abstract should be up to 500 words long, with no pictures, photos, equations, tables, - text only.

Povzetek: - Abstract in Slovenian language.

Main text should be structured logically in chapters, sections and sub-sections. Type of letters is Calibri, 10pt, full justified.

Units and abbreviations: Required are SI units. Abbreviations must be given in text when first mentioned.

Proofreading: The proof will be send by e-mail to the corresponding author in MS Word's Track changes function. Corresponding author is required to make their proof corrections with accepting or rejecting the tracked changes in document and answer all open comments of proof reader. The corresponding author is responsible to introduce corrections of data in the paper. The Editors are not responsible for damage or loss of submitted text. Contributors are advised to keep copies of their texts, illustrations and all other materials.

The statements, opinions and data contained in this publication are solely those of the individual authors and not of the publisher and the Editors. Neither the publisher nor the Editors can accept any legal responsibility for errors that could appear during the process.

Copyright: Submissions of a publication article implies transfer of the copyright from the author(s) to the publisher upon acceptance of the paper. Accepted papers become the permanent property of "Journal of Energy Technology". All articles published in this journal are protected by copyright, which covers the exclusive rights to reproduce and distribute the article as well as all translation rights. No material can be published without written permission of the publisher.

Chapter examples:

1 MAIN CHAPTER (Arial bold, 12pt, after paragraph 6pt space)

1.1 Section (Arial bold, 11pt, after paragraph 6pt space)

1.1.1 Sub-section (Arial bold, 10pt, after paragraph 6pt space)

Example of Equation (lined 2 cm from left margin, equation number in normal brackets (section.equation number), lined right margin, paragraph space 6pt before in after line):

Equation (1.1)

Tables should have a legend that includes the title of the table at the top of the table. Each table should be cited in the text.

Table legend example:

Table 1: *Name of the table (centred, on top of the table)*

Figures and images should be labelled sequentially numbered (Arabic numbers) and cited in the text – Fig.1 or Figure 1. The legend should be below the image, picture, photo or drawing.

Figure legend example:

Figure 1: *Name of the figure (centred, on bottom of figure, photo, or drawing)*

References

- [1] **N. Surname:** *Title*, Journal Title, Vol., Iss., p.p., Year of Publication
- [2] **N. Surname:** *Title*, Publisher, Year of Publication
- [3] **N. Surname:** *Title* [online], Publisher or Journal Title, Vol., Iss., p.p., Year of Publication. Available: website (date accessed)

Examples:

- [1] **J. Usenik:** *Mathematical model of the power supply system control*, Journal of Energy Technology, Vol. 2, Iss. 3, p.p. 29 – 46, 2009
- [2] **J. J. DiStefano, A.R. Stubberud, I. J. Williams:** *Theory and Problems of Feedback and Control Systems*, McGraw-Hill Book Company, 1987
- [3] **T. Žagar, L. Kegel:** *Preparation of National programme for SF and RW management taking into account the possible future evolution of ERDO* [online], Journal of Energy Technology, Vol. 9, Iss. 1, p.p. 39 – 50, 2016. Available: [http://www.fe.um.si/images/jet/Volume 9 Issue1/03-JET_marec_2016-PREPARATION OF NATIONAL.pdf](http://www.fe.um.si/images/jet/Volume%209%20Issue1/03-JET_marec_2016-PREPARATION_OF_NATIONAL.pdf) (7. 10. 2016)

Example of reference-1 citation: In text [1], text continue.

Nomenclature

(Symbols)	(Symbol meaning)
t	time

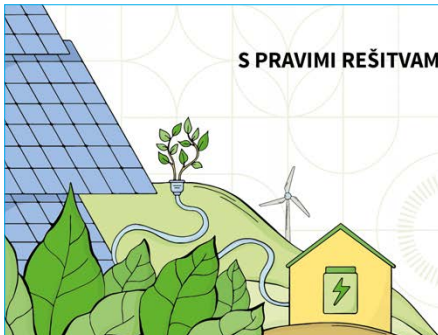


REPUBLIKA SLOVENIJA
MINISTRSTVO ZA VISOKO ŠOLSTVO,
ZNANOST IN INOVACIJE



S PRAVIMI REŠITVAMI DO ENERGETSKE IN STROŠKOVNE UČINKOVITOSTI

Zmanjševanje rabe energije, stroškov in emisij z razvojem, financiranjem in izvedbo projektov na področju energetske učinkovitosti, obnovljenih virov in trajnostne mobilnosti.



Zavod Energetskega agencija za
Savinjsko Šaleško in Koroško
Koroška cesta a37a, 3320 Velenje



Fakulteta za energetiko

Krško - Velenje



- > osebni pristop
- > redni in izredni študij
- > visoka zaposljivost diplomantov

- I. VS, UN
- II. MAG
- III. DR



Priključi se tudi ti!

www.fe.um.si



**MI SPREMINJAMO
PREMIKAMO
RASTEMO**

#EU Green Leaf

**VELENJE JE V LETU 2024 NOSILEC NAZIVA
EVROPSKI ZELEN LIST,**

član Misije 100 podnebno nevtralnih mest in
nosilec naziva Slovenia Green Gold.



**MESTNA
OBČINA
VELENJE**

WWW.VELENJE.SI



FAKULTETA ZA
VARSTVO
OKOLJA

ŠTUDIJSKA PROGRAMA VARSTVO OKOLJA
IN EKOTEHNOLOGIJE

POSTANI

**diplomirana ekotehnologinja /
diplomirani ekotehnolog
magistrica ekotehnologinja /
magister ekotehnolog**



OKOLJE VARUJEMO Z ZNANJEM.

FAKULTETA ZA VARSTVO OKOLJA

VAŠ PARTNER PRI TRAJNOSTNEM RAZVOJU

- Podpora pri razvoju okolju prijaznih izdelkov z orodji ekodizajna
- LCA analize
- Izračun izdelčnih in organizacijskih ogljičnih odtisov
- Priprava strategij razogljčenja
- Priprava strategij za krožno gospodarstvo
- Priprava poročil o trajnosti skladno z ESRS
- Priprava strategij trajnostnega razvoja
- Monitoringi dvoživk
- Poročila o vplivih na okolje
- Okoljska poročila
- Poročila o stanju okolja
- Občinski programi varstva okolja
- Demografske študije
- Izobraževanja s področja trajnostnega razvoja

Izkušeno strokovno skupino najdete na:

Trg mladosti 7 | Velenje | 03 898 64 10 | info@fvo.si | www.fvo.si



HIDROELEKTRARNE NA SPODNJI SAVI



Hidroelektrarne na Spodnji Savi, d.o.o.
Cesta bratov Cerjakov 33A, 8250 Brežice
T: +386 7 49 92 860
F: +386 7 49 92 880
E: info@he-ss.si // W: www.he-ss.si



VARJENJE
WELDING



LASERSKI RAZREZ
LASER CUTTING



STISKANJE PLOČEVINE
COMPRESSION OF SHEET METAL



KRIVLJENJE PLOČEVINE
SHEET METAL BENDING



STRUŽENJE IN REZKANJE
TURNING AND MILLING



POVRŠINSKA OBDELAVA
SURFACE TREATMENT

SKITTI d.o.o.
Podlipovica 27z, 1411 Izlake, Slovenija
+386 (0)56 79 660

PE KISOVEC
Loke pri Zagorju 14b,
1412 Kisovec, Slovenija
+386 (0)56 49 650

info@skitti.si , www.skitti.si

Skitti

LASERSKI RAZREZ
IN PROIZVODNJA
KOVINSKIH IZDELKOV

LASER CUTTING AND
METAL FABRICATION



Dravske elektrarne Maribor

Skupina hse



www.dem.si

Dravske elektrarne Maribor

Z osmimi velikimi hidroelektrarnami na reki Dravi, s petimi malimi hidroelektrarnami in petimi sončnimi elektrarnami družba Dravske elektrarne Maribor proizvede skoraj četrtino vse slovenske električne energije. Učinkovitost, zanesljivost, prilagodljivost, celovitost ter okoljska in družbena odgovornost so temeljne vrednote družbe, ki jim sledimo pri obstoječih zmogljivostih in tistih, ki jih še nameravamo zgraditi.

RAZVOJNI PROJEKTI TEŠ/HSE

VODIKOVE
TEHNOLOGIJE



SOPROIZVODNJA
TOPLOTE IN
ELEKTRIKE IZ
BIOMASE



PLAVAJOČA
SONČNA
ELEKTRARNA



ZAJEM IN UPORABA
CO2 (CCS/CCU)



PRETVORBA OGLJIKOVODIKOV
(V SINTETIČNE PLINE, GORIVA)



PLINSKO-PARNA
ELEKTRARNA -
NADGRADNJA

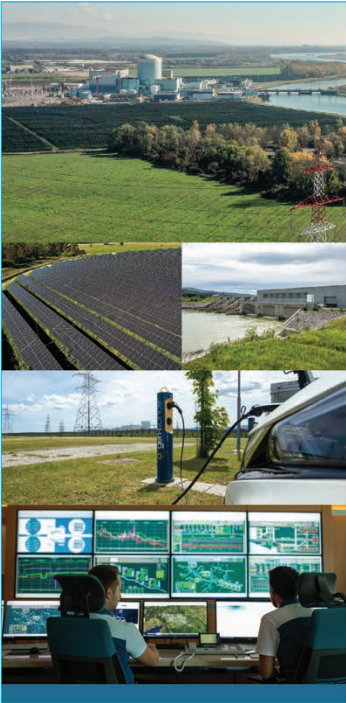


PREOBRAZBA
DALJINSKEGA
OGREVANJA



TEHNOELEKTRARNA
SOŠTANJ

Skupina hse



gen
S K U P I N A



Proizvajalec in dobavitelj nizkoogljične energije **za zanesljivo oskrbo odjemalcev**



Vodilni investitor in razvijalec **jedrsk**e tehnologije v Sloveniji



Promotor in **investitor v obnovljive vire energije** in napredne energetske storitve

ODGOVORNA ENERGIJA

gen-energija.si



ISSN 1855-5748



9 771855 574008